

Organoids and organ chips in ophthalmology

Navid Manafi, Fereshteh Shokri, Kevin Achberger, Masatoshi Hirayama, Melika Haji Mohammadi, Farsad Noorizadeh, Jiaxu Hong, Stefan Liebau, Takashi Tsuji, Peter M.J. Quinn, Alireza Mashaghi

PII: S1542-0124(20)30171-3

DOI: <https://doi.org/10.1016/j.jtos.2020.11.004>

Reference: JTOS 583

To appear in: *Ocular Surface*

Received Date: 24 August 2020

Accepted Date: 12 November 2020

Please cite this article as: Manafi N, Shokri F, Achberger K, Hirayama M, Mohammadi MH, Noorizadeh F, Hong J, Liebau S, Tsuji T, Quinn PMJ, Mashaghi A, Organoids and organ chips in ophthalmology, *Ocular Surface* (2020), doi: <https://doi.org/10.1016/j.jtos.2020.11.004>.

This is a PDF file of an article that has undergone enhancements after acceptance, such as the addition of a cover page and metadata, and formatting for readability, but it is not yet the definitive version of record. This version will undergo additional copyediting, typesetting and review before it is published in its final form, but we are providing this version to give early visibility of the article. Please note that, during the production process, errors may be discovered which could affect the content, and all legal disclaimers that apply to the journal pertain.

© 2020 Published by Elsevier Inc.

1 **Title: Organoids and organ chips in ophthalmology**

2 **Authors:** Navid Manafi^{1,2,†}, Fereshteh Shokri^{3,†}, Kevin Achberger⁴, Masatoshi Hirayama^{5,6},
3 Melika Haji Mohammadi¹, Farsad Noorizadeh⁷, Jiaxu Hong^{1,8,9,10}, Stefan Liebau⁴, Takashi
4 Tsuji^{11,12}, Peter M.J. Quinn^{13,14*}, Alireza Mashaghi^{1*}

5 ¹Medical Systems Biophysics and Bioengineering, The Leiden Academic Centre for Drug
6 Research (LACDR), Leiden University, 2333CC Leiden, The Netherlands

7 ²Max Rady College of Medicine, University of Manitoba, Winnipeg, Canada

8 ³Department of Epidemiology, Erasmus Medical Center, Rotterdam, The Netherlands

9 ⁴ Institute of Neuroanatomy & Developmental Biology (INDB), Eberhard Karls University
10 Tübingen, Österbergstrasse 3, 72074 Tübingen, Germany

11 ⁵ Department of Ophthalmology, Tokyo Dental College Ichikawa General Hospital,
12 Chiba, 272-8513, Japan

13 ⁶ Department of Ophthalmology, School of Medicine, Keio University, Tokyo, 160-8582, Japan

14 ⁷ Basir Eye Health Research Center, Tehran 1418643561, Iran

15 ⁸ Department of Ophthalmology and Visual Science, Eye, and ENT Hospital, Shanghai Medical
16 College, Fudan University, 83 Fenyang Road, Shanghai, China

17 ⁹ Key NHC Key Laboratory of Myopia (Fudan University); Laboratory of Myopia, Chinese
18 Academy of Medical Sciences, Shanghai, China

19 ¹⁰ Key Laboratory of Myopia, National Health and Family Planning Commission, Shanghai,
20 China

21 ¹¹ Laboratory for Organ Regeneration, RIKEN Center for Biosystems Dynamics Research,
22 Hyogo, 650-0047, Japan

23 ¹² Organ Technologies Inc., Minato, Tokyo, 105-0001, Japan

24 ¹³ Jonas Children's Vision Care and Bernard & Shirlee Brown Glaucoma Laboratory, Columbia
25 Stem Cell Initiative, Departments of Ophthalmology, Pathology & Cell Biology, Institute of
26 Human Nutrition, Vagelos College of Physicians and Surgeons, Columbia University. New
27 York, New York, USA

28 ¹⁴ Edward S. Harkness Eye Institute, Department of Ophthalmology, Columbia University Irving
29 Medical Center – New York-Presbyterian Hospital, New York, NY, USA

30 † Co-first authors

31 **Co-corresponding authors:**

32 Peter M.J. Quinn, Edward S. Harkness Eye Institute, Department of Ophthalmology, Columbia
33 University Irving Medical Center – New York-Presbyterian Hospital, New York, NY, USA,
34 pq2138@cumc.columbia.edu

35 Alireza Mashaghi, Medical Systems Biophysics and Bioengineering, The Leiden Academic
36 Centre for Drug Research (LACDR), Leiden University, 2333CC Leiden, The Netherlands,
37 a.mashaghi.tabari@lacdr.leidenuniv.nl

38

39

40

41

42

43

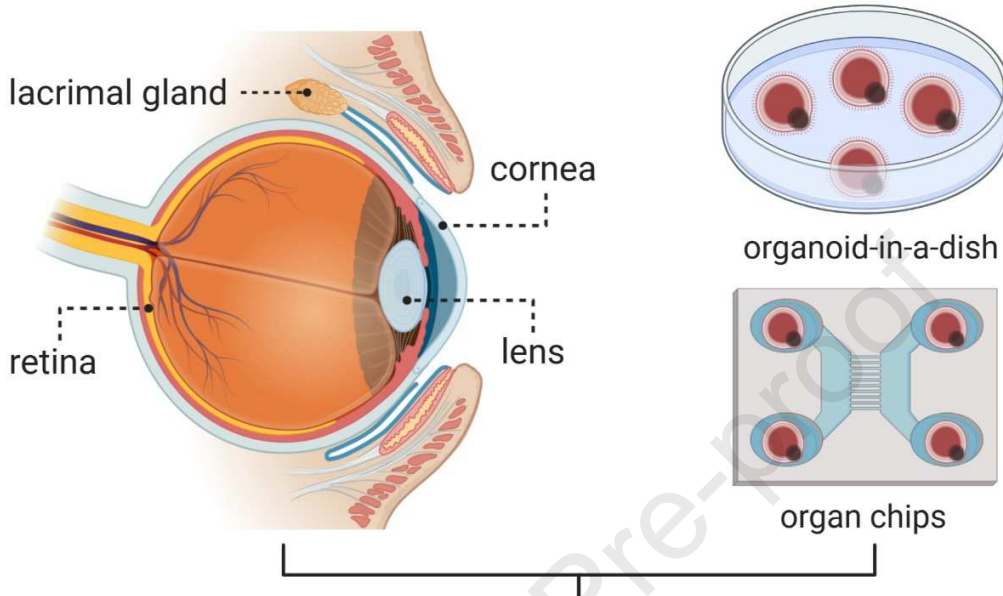
44

45

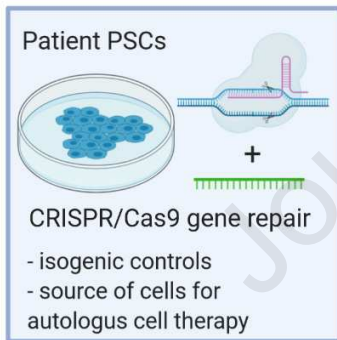
46

47 **Graphical Abstract:**

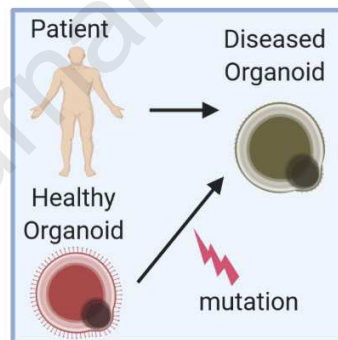
Eye Tissue Organoids and Organ Chips



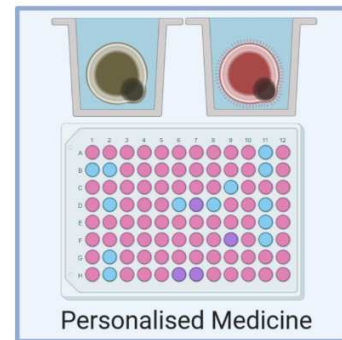
Gene Editing



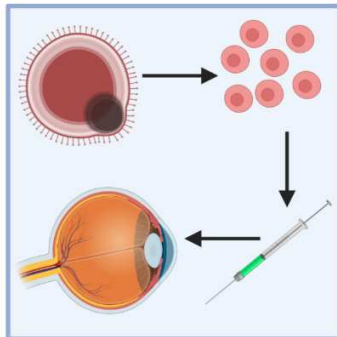
Disease Modeling



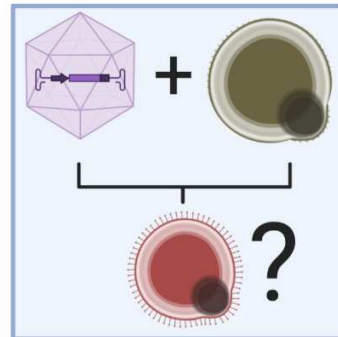
Drug Screening



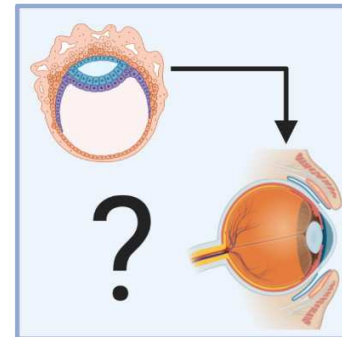
Cell Therapy



Gene Augmentation



Developmental Biology



Abstract:

Recent advances have driven the development of stem cell-derived, self-organizing, three-dimensional miniature organs, termed organoids, which mimic different eye tissues including the retina, cornea, and lens. Organoids and engineered microfluidic organ-on-chips (organ chips) are transformative technologies that show promise in simulating the architectural and functional complexity of native organs. Accordingly, they enable exploration of facets of human disease and development not accurately recapitulated by animal models. Together, these technologies will increase our understanding of the basic physiology of different eye structures, enable us to interrogate unknown aspects of ophthalmic disease pathogenesis, and serve as clinically-relevant surrogates for the evaluation of ocular therapeutics. Both the burden and prevalence of monogenic and multifactorial ophthalmic diseases, which can cause visual impairment or blindness, in the human population warrants a paradigm shift towards organoids and organ chips that can provide sensitive, quantitative, and scalable phenotypic assays. In this article, we review the current situation of organoids and organ chips in ophthalmology and discuss how they can be leveraged for translational applications.

Keywords: Organoid, organ-on-chip, organ chip, microfluidics, ophthalmology, eye, retina, cornea, lens, lacrimal gland.

Highlights

- Organoids are 3D structures grown from stem cells with organ-level functions.

72

73 • Organ chips have microfluidic channels lined by living human organ-specific cells.

74

75 • Microfluidic organ chips can enhance the significance of organoid models by introducing
76 absent mechanical, structural and anatomical cues

77

78 • Organoids and organ chips have been used to understand eye physiology and model
79 ophthalmic disease.

80

81 • Organoids and organ chips can facilitate the evaluation of therapeutics, e.g. drug
82 screening or gene therapy vectors.

83

84 • Organoids can be used as a source for autologous cell transplantation.

85

86 **Introduction**

87 Loss of vision severely affects the quality of life and is one of the most feared health
88 conditions in society. The demand for basic research on ophthalmic diseases is rising due to the
89 increasing world population and the increase in life expectancy and subsequent rise in the number of
90 cases of ophthalmic diseases such as corneal dystrophy (e.g., Fuchs'), dry eye disease, Sjögren's
91 syndrome, retinitis pigmentosa (RP) and retinoblastoma. Previously, experimental studies have been
92 performed *in vivo* on animal models (from *Drosophila* and zebrafish to rodents and large mammals)
93 or *in vitro* cell culture models [1–3]. These models have contributed to ophthalmology in many ways,
94 including their role in finding basic functional characteristics at the cellular level, modeling eye

95 development, disease pathogenesis, therapy development, and drug screening [4–9]. However, these
96 studies can suffer from limited clinical translatability, for example, due to species differences in the
97 tropism of viral vectors or the transcriptome for both protein-coding and non-coding transcripts [10–
98 12]. The commonly used *in vitro* models often fail to reproduce organ-level functionality, which is
99 needed for realistic disease modeling. Therefore, more representative models of human eye tissues
100 are required [13].

101 In response to this need, two new technologies have been recently developed: organoids
102 and organ-on-chips (organ chips) [13,14]. Organoids are stem cell-derived, three-dimensional
103 assemblies that consist of organ-specific cell types that self-organize through cell sorting and
104 spatially restricted lineage commitment, thus mimicking the architectural and functional
105 complexity of native organs [15]. Organoids are derived from embryonic stem cells (ESCs),
106 induced pluripotent stem cells (iPSCs), or organ-restricted adult stem cells (aSCs). During stem
107 cell differentiation, temporal manipulation of the *in vitro* microenvironment through
108 supplementation with exogenous components such as growth factors, small molecules, and
109 extracellular matrix (ECM) substrates can simulate conditions of the fetal microenvironment, and
110 improve organoid differentiation and maturation [15]. Another evolving model is organ chip
111 technology, which combines the uses of microfluidic technology, biomaterials, and cell culture
112 techniques to model human-like organs on a micro-scale. Organ chips are microchips designed to
113 recapitulate the microarchitecture and function of living human organs. Commonly, organ chips
114 are transparent, contain varying hollow microfluidic channels and cell compartments which can
115 be lined by living human organ-specific cells. External artificial forces can be applied to mimic
116 the physical microenvironment of the living organs. Organoids and organ chips have been
117 developed to model many organs, including the gut, liver, kidney, brain, and more recently, eye

118 structures including the retina, cornea, and lens [16]. In this article, we discuss the use of
119 organoids and organ chips in ophthalmology. We review the use of these techniques to study eye
120 development and physiology, disease mechanisms, and the development of diagnostic assays and
121 therapeutics for personalized medicine.

122

123 **Cornea**

124 The cornea is the transparent outermost layer of the eye that is responsible for focusing
125 most of the incoming light and is thus essential for vision. Over the last decades, efforts have
126 been made to create in vitro corneal models. In 1993 Minami et al. succeeded in reconstructing
127 the three layers of the cornea (endothelium, stroma, and epithelium) from cells isolated from
128 bovine cornea tissues [17]. The three layers were engineered sequentially on top of each other,
129 with the epithelial layer interfacing a liquid/air matrix. A similar approach was employed to
130 develop the 3-dimensional corneal model derived from human cells by Germain et al., that
131 reconstructed corneas by culturing epithelial cells on collagen gels containing fibroblasts [18].
132 Griffith et al. fabricated a human corneal model employing human corneal cell lines. They found
133 that their model resembled the human cornea in morphology, transparency, and histology. The
134 model responded to both stromal swelling and corneal wound healing to a degree similar to post-
135 mortem cornea [19]. The efforts to develop the 3D cornea model entered a new phase with the
136 introduction of organoid technology and chip-based modeling. In what follows, we discuss
137 corneal organoids and cornea chips, and then describe their applications to drug studies.

138

139 **Corneal organoids**

140 Corneal organoids are 3D cornea models designed to be suitable for developmental
141 studies, modeling of some cornea disorders, and possibly organ replacement purposes [20].
142 Organoids are generated from embryonic stem cells (ESCs) and induced pluripotent stem cells
143 (iPSCs) that differentiate into various cornea cells [21–24].

144 In a breakthrough study, Foster et al. used human iPSCs to develop corneal organoids.
145 These organoids contained three cell types of the cornea - epithelium, stromal keratocytes, and
146 the endothelium. These structural features were characterized using immunofluorescence
147 staining for epithelial markers (KRT3, KRT14, and p63), stromal keratocytes (CD34), and
148 endothelial markers (COL8A1, F11R, S100A4). In addition, these organoids consisted of
149 extracellular matrix collagens and proteoglycan core proteins which are essential components of
150 the stromal matrix. TEM and immunofluorescence staining showed different matrix proteins and
151 organized protein fibrils in different layers of the organoids. While the outer layers contained
152 perlecan and collagen type VIII, the deeper layers stained for stromal proteins LUM and KERA,
153 Collagen types I and V [25].

154 Shortly after the development of corneal organoids by Foster et al. a new protocol was
155 developed by Susaimanickam et al., which generated, using a simpler and more efficient culture
156 method, more complex 3D corneal organoids and even, in rare cases, whole eyeball-like
157 structures. In this protocol, either human ESCs or human iPSCs are cultured *in situ* in retinal
158 differentiation medium (RDM), with the absence of noggin. After four weeks in culture, the stem
159 cells had differentiated in eye field primordial clusters (EFPs). They found that continued *in situ*
160 differentiation of these EFPs in RDM led to the formation of lens epithelial clusters, ocular
161 surface epithelium, and optic cups. Interestingly, they found that in rare cases the EFPs gave rise
162 to 3D miniature eyeballs, including an anterior transparent cornea primordium surrounded by the

163 neuroretinal cup. At two weeks of suspension culture, the EFPs gave rise to both retinal and
164 corneal primordia. At this point, the corneal primordia regions were lifted and cultured in the
165 corneal differentiation medium (CDM) for further maturation. Six to eight weeks after culturing
166 the corneal primordia gave rise to minicorneas. Subsequent examination of these minicorneas
167 showed prevalent corneal morphological structures and expressed cornea-specific markers [26].

168 These corneal organoids open up possibilities for multiple downstream applications that
169 are unattainable using current *in vitro* culture systems.

170

171 Cornea chip

172 Engineering cornea mimics on chips is still at its infancy. A few steps have been taken
173 towards modeling cornea; despite their simplicity, current cornea chips are already able to
174 recapitulate certain disease features. Puleo et al. made the first attempt to culture cornea cells in
175 microfluidic devices in 2009 [27]. They succeeded in developing a bilayer structure containing a
176 corneal epithelial layer and a layer of stromal cells on a collagen vitrigel substrate. The model
177 was then used to measure transepithelial permeability. Nearly a decade later, Bennet et al.
178 developed a cornea chip that included epithelial layers, basement membrane, and Bowman's
179 membrane, and importantly, they simulated tear flow dynamics in their microfluidic device [28].
180 They used immortalized human corneal epithelial cells (hTCEpi) and cultured them on a
181 Polydimethylsiloxane (PDMS) membrane. They found that cells seeded on a fibronectin-coated
182 membrane were more viable compared to uncoated or collagen-coated membranes. The
183 permeability of the epithelium underflow closely resembled *in vivo* conditions.

184 A significant breakthrough in the development of an ocular surface chip was the chip
185 development by Seo et al. that integrated both cornea and conjunctiva structures in one platform

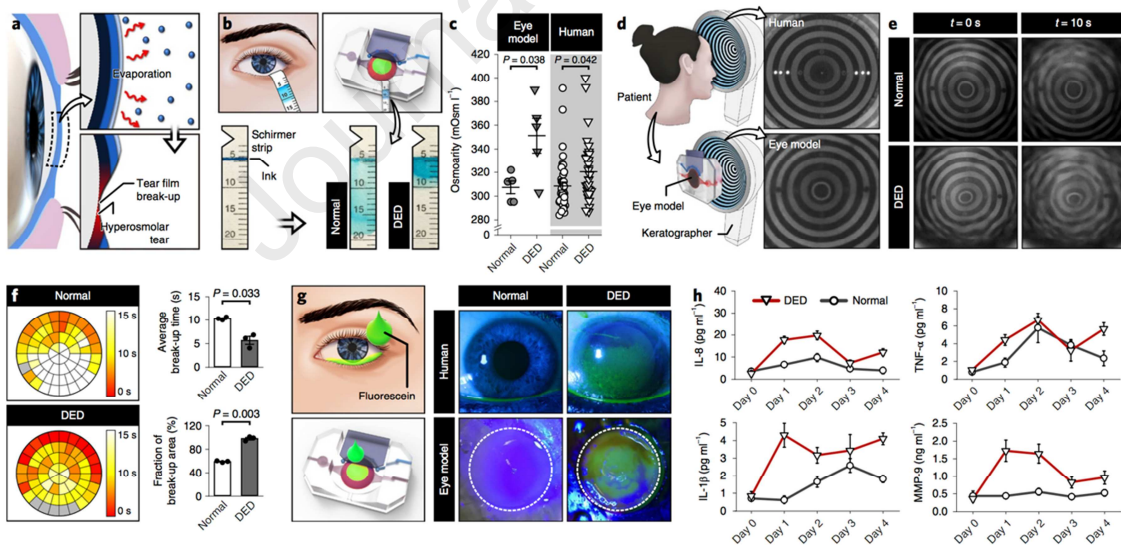
186 and interfaced them with a blinking eyelid [14]. They developed a dome-shaped scaffold with a
187 perfusion system and an eyelid mimic that is actuated to slide on the scaffold. The cornea mimic
188 included epithelial cells with primary human keratocytes embedded in a hydrogel to mimic the
189 stroma. Using a 3D patterning approach, concentric patterns of the conjunctiva (including
190 epithelial and goblet cells) and cornea structures were fabricated. The structure, however, lacked
191 vasculature and immune cells that are present in the conjunctiva *in vivo*.

192 The ocular surface chip developed by Seo et al. recapitulated important anatomical and
193 physiological properties of human counterparts [14]. Stratified epithelium in this device is
194 composed of 7-8 layers of epithelial cells (similar to *in vivo* conditions) as well as a layer of cells
195 expressing basal cell-specific marker (p63). Similarly, the engineered conjunctiva contained
196 multiple epithelial layers and showed the expression of key biochemical markers. Importantly,
197 the tissue could produce mucin proteins. An essential aspect of this design is that the model
198 incorporates key mechanical processes including blinking with physiological frequencies (e.g.,
199 0.2 Hz) as well as tear film dynamics. The tear secretion rate of the device was properly tuned to
200 its natural values, and a drainage system for tear excess was designed. This ensured the
201 maintenance of a very thin and uniform tear film of approximately 6 μm thickness (within the
202 range of *in vivo* values), as shown by optical coherence tomography. The blinking process was
203 shown to be noninvasive to the ocular surface and did not lead to scarring. The mechanical shear
204 was shown to promote cellular differentiation in the epithelial layer, indicating that the eyelid is
205 more than just a “lid” and the mechanical forces are sensed and responded to by the cellular
206 biochemical network.

207 Ocular surface chips remained to be adapted and used as disease models. The only major
208 development in this direction was the engineering of a Dry Eye Disease (DED) model on the

209 platform developed by Seo et al. [14]. By reducing the frequencies of blinking from 12 to 6 times
 210 per minute and adjusting the humidity of the environment allows for the simulation of an
 211 evaporative DED model. Reduced blinking frequency leads to changes in tear osmolality and
 212 film instability, as shown by break-up time estimation. Importantly, these DED related
 213 biomechanical changes led to cellular changes seen in DED *in vivo*. For example, inflammatory
 214 cytokines such as interleukin 1β , $TNF\alpha$, and matrix metalloproteinase (MMP)-9 were
 215 overexpressed upon the reduction of blinking frequency in the chip. Overall, this proof-of-
 216 concept study demonstrates that the chip model can capture the mechanical and biochemical
 217 features of DED (Fig. 1). These results are highly promising and set the stage for the
 218 development of chip-based models for other ocular surface diseases. For this aim, one may have
 219 to incorporate additional complexities e.g. the immune system and vasculature.

220



221

222 *Figure 1: Dry eye disease chip. a) Evaporation induced break-up of the tear film and increase of*
 223 *tear osmolality together lead to a loss of homeostasis. b) Absorption of tears into the Schirmer*
 224 *strips in the healthy and DED models. Tear absorption is visualized by the smearing of the blue*

225 ink within the strips. c) Tear osmolarity in the DED (closed triangle) and the healthy (closed
226 circle) models. Human clinical data of osmolarity are from healthy (open circle) and DED
227 subjects (open triangle). d) Keratographs showing concentric rings projected on the human
228 ocular surface (top) and the engineered ocular surface (bottom). e) Representative images of
229 projected ring patterns on the engineered ocular surface of the healthy (top row) and the DED
230 (bottom row) groups captured at $t = 0$ s (left column) and $t = 10$ s (right column). f) Spatial
231 mapping of tear film break-up time in the normal (top) and the DED (bottom) models. Different
232 colors in the representative circular heat maps indicate different tear break-up times. g)
233 Fluorescein staining of the eye model and human subjects. h) Concentrations of inflammatory
234 mediators (IL-8, TNF- α , IL-1 β , and MMP-9) in the normal (circle) and the DED (triangle)
235 groups plotted against the duration of culture. The figure is taken from Jeongyun Seo et al. with
236 permission [14].

237

238 Applications to drug studies

239 Cornea chips have been used to study pharmacokinetics and preclinical drug evaluation.
240 Bennet et al. performed a drug study on their model with Pred Forte (Prednisolone 1%) and
241 Zaditor (Ketotifen) to assess the functionality of their model in drug permeability [28]. They
242 found that the pulsatile tear flow had the most similarity to the human eye than the continuous
243 flow or static condition [28]. Their findings were correlated with the formulation of the drug and
244 mode of the action of the chip (static or with the flow) so that it would be a representative model
245 of the human cornea *in vitro* [28]. Unfortunately, pharmacological immunomodulation ocular
246 surface cannot be accurately mimicked using current chip designs, as these designs lack the
247 immune system. However, nonimmunological processes can be drugged effectively in chip

248 models of ocular surface inflammatory diseases. An example of such a study is the analysis
249 conducted on the DED model of Seo et al. [14]. They exposed the DED model to endogenous
250 lubricin to assess whether the findings of this in vitro model are comparable with clinical
251 outcomes. The results not only showed increased break-up time and decreased area of the film
252 tear rupture but also changed corneal fluorescein staining resembling what was found in the
253 clinical trials. This analysis shows the values of cornea chips, as these “clinical” measurements
254 are now possible at the preclinical stages of drug analysis, thanks to the chip technology.
255 Furthermore, the DED model was used to discover the therapeutic effect of lubricin at the
256 molecular scale. Concentration profiles of inflammatory factors such as toll-like receptor-4
257 (TLR-4) of IL-8, TNF- α , IL-1 β , and MMP-9 can be measured in the tear film. The DED model
258 showed a marked decrease in inflammatory markers upon lubricin administration, in agreement
259 with the findings of clinical trials.

260 One important issue in drug assays on cornea chips relates to drug permeation and accessibility
261 to ocular surface layers. Bai et al. created a cornea chip model to determine dextran diffusion
262 permeability across the corneal barriers [29]. They used dextran with several distinct molecular
263 weights ranging from 10kDa to 70kDa to simulate drug diffusion across cornea layers and to
264 measure permeability. They found that epithelium is a major determinant of drug transportation
265 rates. Future studies are needed to investigate the translational value of these drug transport data.
266 This is because the proof-of-concept analysis by Bai et al. was based on mouse cornea cells and
267 did not include the cellular complexity of human cornea and its collagen content precisely.

268

269 **Lacrimal glands**

270 The lacrimal glands (LGs) secrete tear fluids, which contain water, electrolytes, and
271 various secreted substances to the ocular surface. Tears play physiologically important roles in
272 maintaining the homeostatic environment on the ocular surface epithelium, such as lid
273 lubrication, hydration, antimicrobial activity, and protection of the ocular surface epithelium.
274 Tear shortage from LGs, which is induced by aging and various pathological conditions, causes
275 dry eye disease (DED). DED is defined at TFOS/DEWS II as a multifactorial disease of the
276 ocular surface characterized by a loss of homeostasis of the tear film, and accompanied by ocular
277 symptoms, in which tear film instability and hyperosmolarity, ocular surface inflammation and
278 damage, and neurosensory abnormalities play etiological roles. Recently, a therapeutic concept
279 of functional lacrimal gland restoration using regenerative medicine, including organoids from
280 pluripotent stem cells, has emerged as a possible way to treat severe DED.

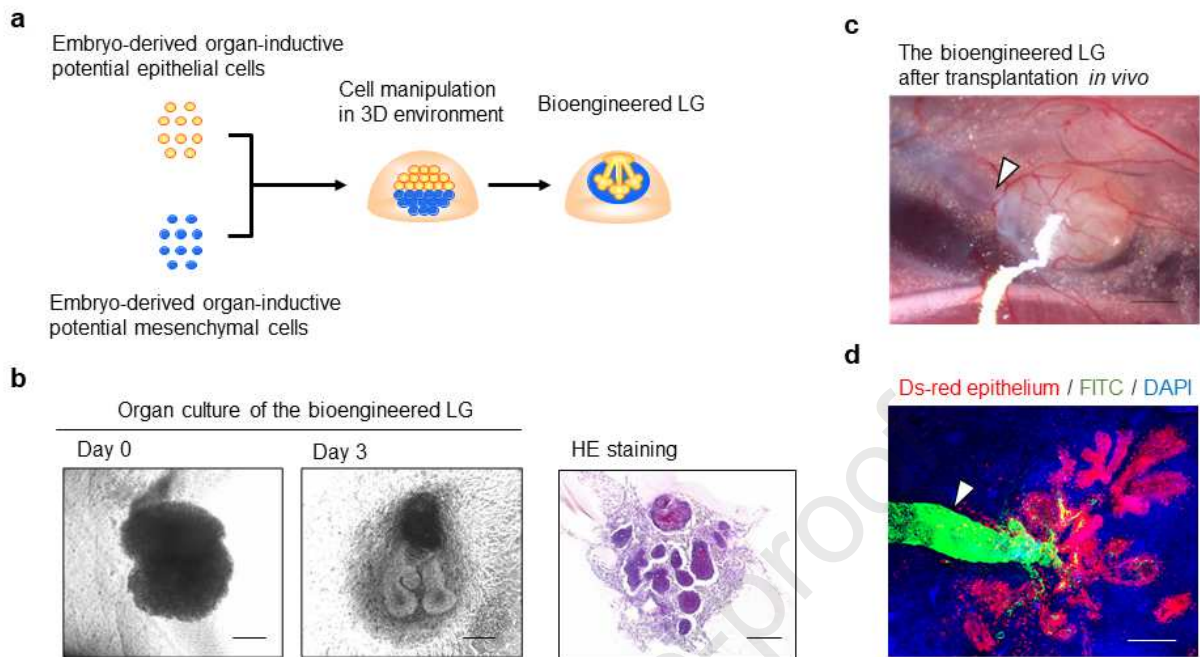
281

282 **Lacrimal gland organoids**

283 One of the challenges for the lacrimal gland regeneration is to reconstruct secretory gland
284 structures and coordinated organ systems with peripheral tissues, such as nerves and blood
285 vessels, because organogenesis requires a complex process involving tissue self-organization,
286 cell-cell interactions, signaling with various molecules for correct cell differentiation to form
287 organs [30][31]. A method in biotechnology based on knowledge from developmental biology
288 for 3D stem cell manipulation *in vitro*, which is designated to mimic organ germ formation
289 during organogenesis, allowed us to generate bioengineered organ germs, including teeth, hair
290 follicle, and salivary glands and LGs, by using embryo-derived organ inductive stem cells (Fig.
291 2a) [32][33][34][35][36][37]. The bioengineered lacrimal gland germs, which were generated
292 with compartmented cells of epithelial and mesenchymal stem cells isolated from mouse lacrimal

293 gland germs in a collagen gel, initiate developmental processes involving the self-organization
294 and multiple cellular assembling to form tubule-alveolar structures *in vitro* (Fig. 2b). The
295 bioengineered lacrimal gland germs achieve mature lacrimal gland structures and recapitulate
296 their connection with peripheral tissues and innervation for fully tear-secretion functions after
297 orthotopic engraftment *in vivo* (Fig. 2c, 2d). As reported in the bioengineered teeth regeneration
298 study, the development of a method to mature the bioengineered lacrimal gland germs *in vitro*,
299 which can immediately function the bioengineered organs *in vivo*, will contribute to lead future
300 organ replacement therapy for DED [34]. These studies have demonstrated that the functional
301 bioengineered lacrimal glands for organ replacement therapy can be achieved by reproduction of
302 the developmental process of LGs in organogenesis.

303 An organoid as a partially functional mini-organ can be generated by using specific
304 developmental gene expression and cytokine signaling, which induce self-organized body
305 patterning and subsequent organ-forming field from pluripotent stem cells.
306 [38][39][40][41][42][43]. Recently, fully functional salivary glands from mouse ES cells have
307 been generated through the induction of organ-forming field (the oral ectoderm; for the salivary
308 glands) with the expression of specific genes for salivary gland development [44]. In the field of
309 the lacrimal gland regeneration, a set of transcription factors, which plays a role in the lacrimal
310 gland development, has been clarified to induce the organ-forming field and signaling for the
311 lacrimal gland organoids [45][46]. As well as the possibility of tissue stem cell injection therapy
312 reported previously [47], the further development of this method of organoid technology for LGs
313 will contribute to the realization of lacrimal gland regenerative medicine.



314
 315 *Figure 2. Development of the bioengineered lacrimal glands in vitro and in vivo. (a)*
 316 *Functional lacrimal gland regeneration using mouse embryo-derived organ-inductive stem cells*
 317 *in the 3D culture environment. (b) Organogenesis of the bioengineered lacrimal glands with*
 318 *branching morphogenesis in vitro (left and center panels) and an image of HE staining of the*
 319 *bioengineered lacrimal gland (right panel). scale bar, 200 μ m. (c) Functional lacrimal gland*
 320 *replacement after orthotopic transplantation in vivo. Arrowhead shows the connection between*
 321 *the host lacrimal excretory duct and the bioengineered lacrimal gland. Scale bar, 500 μ m. (d)*
 322 *The bioengineered lacrimal glands developed with full functionality. Ds-red expressing*
 323 *epithelium achieved acini and duct structures. FITC gelatin (green), which was injected from the*
 324 *host lacrimal excretory duct, reached to the bioengineered lacrimal gland. Arrowhead shows the*
 325 *connection between the host lacrimal excretory duct and the bioengineered lacrimal gland. Scale*
 326 *bar, 200 μ m. The figures were reprinted from [48].*

327

328 **Lacrimal gland chips**

329 Various innovations in bioengineering have been applied to regenerate functional organs to treat
330 or modeling diseases. For example, artificial regulation of tear secretion from LGs by stimulating
331 neural pathways using medical devices has been proposed [49]. To generate complex secretory
332 gland structure, previous reports have used biohybrid materials, such as a decellularized scaffold,
333 for a successful 3D reconstruction of LG [50][51]. Other studies have reported the *in vitro*
334 models of several components of the ocular surface, such as conjunctival tissues and lacrimal
335 gland epithelium [52], individually [53]. The 3D culture environment, including microgravity
336 cell culture and Matrigel culture methods, has been a key to investigate the lacrimal gland
337 function and DED [54][55][56]. A tissue engineering technology for reconstruction of a complex
338 3D organ system (LGs-tear film-ocular surface) has been attempted to build up *in vitro* disease
339 modeling of DED [57]. These studies have indicated that it is effective to create functional tissue
340 mimics, which use a co-culture system of various tissues of tear film-ocular surface system
341 including the lacrimal gland spheroids and conjunctival epithelium, as a model for DED and
342 therapeutic evaluation. The next-generation research of the lacrimal gland regenerative medicine
343 using organoids and organ chips is now expanding as a viable model based on recent exponential
344 advances in developmental biology, stem cell biology, and tissue engineering technology.

345

346 **Retina**

347 **Retinal organoids**

348 The first retinal organoids (ROs) were made from mouse (m)ESCs [13,58]. The Sasai
349 laboratory found that the development of the optic cup is a self-directed process and does not
350 rely on influence from external structures. Their model had the six major types of neurons and
351 one glial cell type of the retina and could recapitulate many aspects of retinal function, including

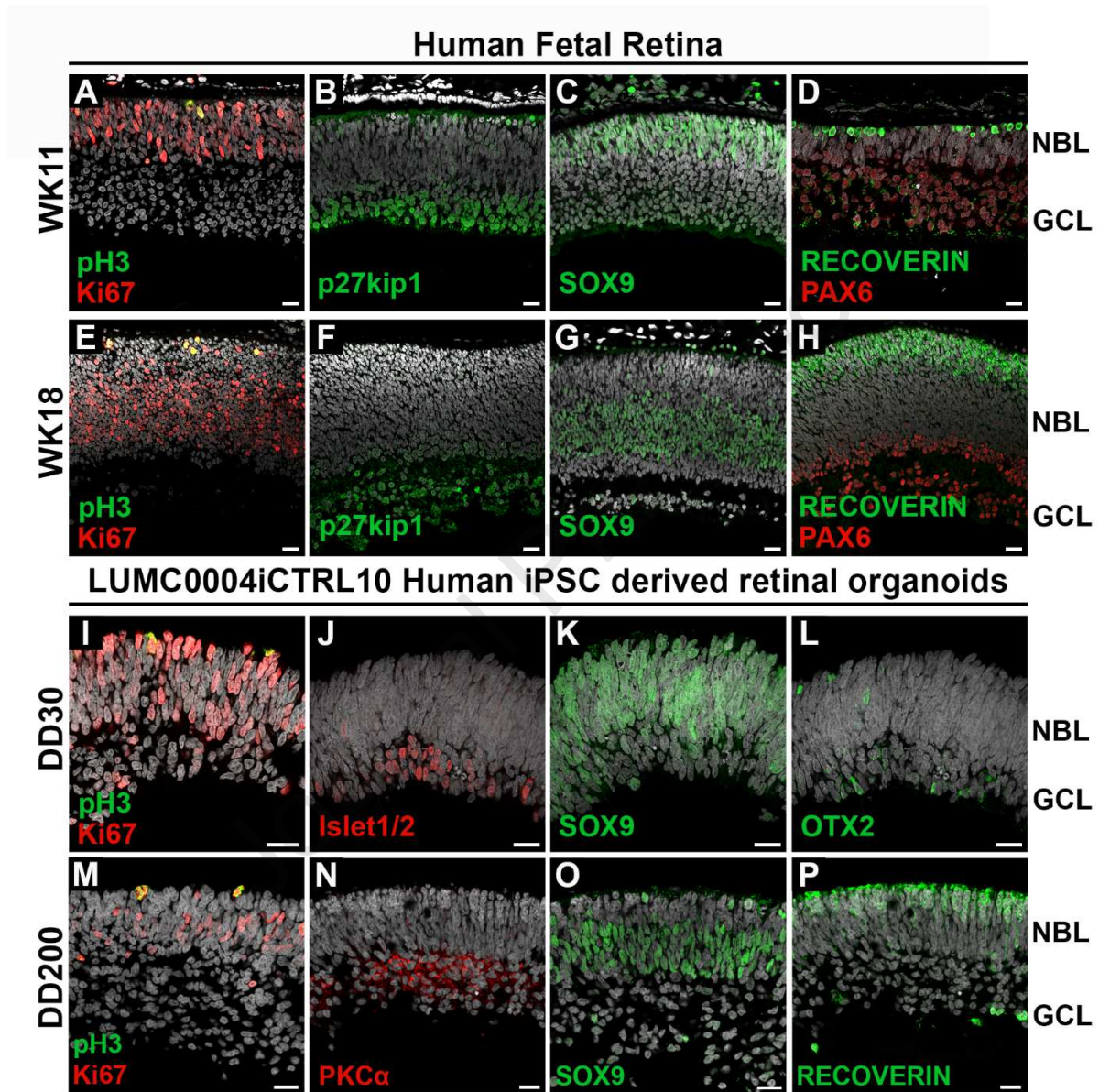
352 morphogenetic movements, interkinetic nuclear migration, and apical-basal polarity [13,58].
353 Although their model was not perfect in recapitulating all facets of the adult mouse retina,
354 including a low percentage of cone photoreceptors, it was a milestone in generating more
355 advanced retinal models that recapitulated *in vivo* characteristics of the mouse retina. Further
356 optimization of their protocol enabled the generation of human (h)ESC-derived ROs for the first
357 time (Nakano et al.) [40]. Compared to the stem cell-derived RO mouse model, the retina derived
358 by this method had longer culture time, which is due to the inherent differences in gestational
359 periods between species. The methodology used was based entirely on a 3D approach relying on
360 extrinsic modulation of cell signaling pathways. Starting from a single cell suspension of hESCs,
361 the cells are seeded in equal numbers in V-bottomed wells of a 96-well plate and undergo quick
362 aggregation to form embryoid bodies (EB). EBs undergo neural induction and form optic
363 vesicles, which are subsequently kept in suspension culture for maturation to laminated ROs
364 [40]. The main alternative to this methodology, popularized by Zhong et al., requires far less
365 extrinsic modulation of cell signaling pathways and proceeds in a mostly self-directed process.
366 Here, hiPSCs are grown to near confluence and made into small floating aggregates, either
367 chemically or mechanically, in suspension to form EBs which undergo neural induction.
368 Subsequent plating of EBs allows for the formation of the retinal neuroepithelium, which can be
369 individually dissected from the bottom of the well, or alternatively, the whole contents of the
370 well can be lifted after mechanically scoring the well in a grid pattern. This is followed by the
371 sorting of ROs for long term suspension culture where they undergo lamination and maturation
372 [59,60]. An alternative to this approach is to let hiPSCs grow to confluence and, instead of
373 generating small floating aggregates, remain as adherent cultures. Removal of FGF2 from the
374 culture medium initiates spontaneous differentiation which is followed by the promotion of

375 neural induction and retinal neuroepithelium formation [61,62]. The methodology by Zhong et
376 al. was the first to show fully laminated 3D iPSC-derived retinal tissue which also yielded more
377 developed outer-segment structures that responded to light stimuli [59]. A third methodology by
378 Lowe et al. used small aggregates of hESCs embedded in Matrigel to form single-lumen
379 epithelial cysts that subsequently adhere to the culture surface forming colonies of retinal
380 progenitors. Dispase treatment promoted lifting of these colonies, which in floating suspension
381 culture formed laminated and maturing retinal organoids [63]. The use of hESCs and hiPSCs
382 has been successfully implemented using all three methodologies, and continued modifications
383 and optimizations are being implemented [40,59,60,64–68]. The retinal architecture of the
384 human fetal retina is recapitulated in hiPSC retinal organoids (Fig. 3).

385 Organoids are useful for understanding the developmental physiology of the retina and its
386 underlying transcriptomic mechanisms. Here, we provide some examples of RO implementation
387 for these purposes. Previously, an essential role of thyroid hormone signaling on cone cell
388 viability and opsin expression has been established. However, the exact mechanism of cone cell
389 differentiation was not known [69]. Retinal organoids have been implemented to further
390 elucidate this mechanism. Eldred et al. found that the retina plays an active role in specifying S
391 or L/M cone subtypes through the temporal expression of thyroid hormone degrading and
392 activating proteins. In early retinal development, thyroid hormone levels are kept low which
393 initiates differentiation to S cones, later in development thyroid hormone levels rise to specify L
394 and M cone cells [70].

395 The organoid models can be used for studying the effect of different genes in eye
396 formation and neuroretina differentiation. Takata et al. studied the effect of *R-spondin 2* (*Rspo2*)
397 and *Sine oculis*-related homeobox 3 (*Six3*) genes [71]. They used *Six3*^{-/-} miPSC-derived and *Six3*

398 conditional knockout (CKO) mESC-derived organoids, finding that Six3-mediated suppression
 399 of *Rspo2* is necessary for neuroretina differentiation and optic vesicle morphogenesis [71].



400

401 *Figure 3. Retinal architecture in the human fetal retina and human iPSC retinal*402 *organoids. Immunohistochemistry pictures of WK11 (A-D) and WK18 (E-H) human fetal retina*403 *and DD30 (I-L) and D200 (M-P) LUMC0004iCTRL10 hiPSC-derived retinal organoids.*404 *Sections were stained with antibodies against: Ki67 (A, E, I, M), pH3 (A, E, I, M), p27kip1 (B,*

405 *F), SOX9 (C, G, K, O), Recoverin (D, H, P), PAX6 (D, H), Islet1/2 (J), PKC α (N), OTX2 (L). In*
406 *human fetal retina at week 11 in the 1st trimester of pregnancy, we observed cycling cells that*
407 *stained positive for anti-Ki67 and spanned the thickness of the neuroblast layer (NBL). The*
408 *mitotic cells located most apically and stained positive for pH3 (A). Inner retinal cells as marked*
409 *by p27kip1 and PAX6 were restricted to the ganglion cell layer and a subset of cells in the NBL*
410 *(B and D). The cells that exited the cell cycle were marked with p27kip1, whereas the ganglion*
411 *cells, amacrine cells, and migrating retinal progenitors were marked with PAX6. Radial glial*
412 *progenitor cell nuclei spanned the thickness of the NBL and stained positive for anti-SOX9 (C).*
413 *Newborn cone photoreceptors marked positive for anti-recoverin (D). In the human fetal retina*
414 *at weeks 18 in the 2nd trimester of pregnancy, we observed the localisation of anti-pH3-positive*
415 *mitotic cells most apically within the NBL (E). However, the cycling anti-Ki67-positive cells*
416 *became mostly restricted to the middle NBL cells but also labeled occasional outer NBL cells*
417 *(E). Both p27kip1- and PAX6-positive cells restricted to the inner NBL and the ganglion cell*
418 *layer (F, H). SOX9-positive cell nuclei localised in the middle NBL and occasionally the outer*
419 *NBL, marking maturing Müller glial cells (G). The outer NBL showed an increase in recoverin-*
420 *positive photoreceptors at week 18 compared to week 11 (H). In early DD30 hiPSC retinal*
421 *organoids we observed that Ki67-positive cycling cells spanned the thickness of the NBL with*
422 *pH3-positive mitotic cells located most apically (I). Ki67-positive cycling cells were also*
423 *detected in the ganglion cell layer (GCL). Islet1/2-positive cells were found mostly restricted to*
424 *the GCL with sporadic cells in the NBL (J). SOX9-positive radial glial progenitor cell nuclei*
425 *spanned the thickness of the NBL but were also seen occasionally in the GCL (K). Immature*
426 *photoreceptors that stained positive for anti- OTX2 could be found in both the NBL and GCL*
427 *(L). In later DD200 hiPSC-derived retinal organoids Ki67-positive cycling cells restricted*

428 *mostly to the middle NBL but occasionally were detected in the outer NBL and in the GCL,*
429 *whereas pH3-positive mitotic cells located apically (M). In the inner retina PKC α -positive*
430 *bipolar cells (N) were detected. SOX9-positive cell nuclei became more restricted to the middle*
431 *NBL but occasionally were detected in the outer NBL and the GCL (O). Recoverin-positive*
432 *photoreceptor cells were mostly restricted to the outer NBL. Some recoverin-positive cells were*
433 *detected within the NBL and occasional recoverin-positive cells were detected in the GCL (P).*
434 *Scale bars: (A-P), 20 μ m. Adapted from Quinn et al. 2019[72] under a creative commons license.*

435
436 Capowski et al. studied the expression pattern of microphthalmia-associated transcription
437 factor (MITF) during differentiation in their hESC-derived optic vesicle model. MITF is a vital
438 regulator of pigmented cell survival and differentiation. They found that in addition to the role of
439 MITF in retinal pigment epithelium (RPE) development, it is also crucial for early optic vesicle
440 cell proliferation.[73] Quinn et al. used hiPSC-derived ROs and human fetal retina to investigate
441 the onset of expression of CRB1 (Crumbs homolog-1) and CRB2 during development and early
442 maturation of the retina [72]. Mutations in CRB1 are associated with a spectrum of retinal
443 dystrophies including RP type 12 and LCA type 8 [74–78]. They found that during the first
444 trimester, CRB2 is the predominant CRB family member. In contrast, the onset of expression of
445 the canonical CRB1 protein at the subapical region coincides with the maturation of the retina
446 during the second trimester. This pattern of CRB1 and CRB2 expression was recapitulated in
447 ROs [72]. To verify that retinal ganglion cells (RGCs) can be identified by the expression of
448 specific surface antigens. Aparicio et al. compared surface antigen expression patterns in the
449 human fetal retina and hESC-derived ROs. They found that CD184 and CD171 were expressed
450 in RGCs from both tissues and that early post-mitotic RGCs express high levels of CD184 while

451 CD171 expression is found in maturing RGCs. These cell surface markers could then be used
452 to purify the RGC population using flow cytometry [79]. RGCs derived from ROs can be used as
453 an effective platform to investigate RGC development, organization, and neurite outgrowth [80].

454 ROs have been used to profile the dynamic transcriptional landscape of retina from early
455 progenitors to differentiated retinal cell types [81–83]. These transcriptomic data have been
456 achieved by using different reporter lines, each assessing a specific type of cell in the human
457 retina. Hereby nine different clusters of cells have been observed during the differentiation of
458 ROs. It has been found that mitotic cells and RGCs decrease over time, rod and cones are formed
459 afterward, and Müller glia increases towards day 200 [84]. Neural retina leucine zipper (NRL) is
460 a gene that has a critical role in rod photoreceptor formation, and patients with NRL mutations
461 exhibit rod degeneration enhanced S-cone syndrome and RP. ROs of null NRL models have also
462 been developed to study the cone photoreceptor development in human-derived ROs [85]. These
463 models can also be useful to assess the transcription factors involved in photoreceptor
464 development.

465 Lastly, in addition to radial glial progenitors, a peripherally located stem cell-like niche
466 called the ciliary marginal zone (CMZ) can contribute to the production of postmitotic cells to
467 the retina in mammals.[76,86–88] The Sasai laboratory used an induction reversal method to
468 generate human ROs with RPE, which contained a CMZ at the boundary between these two
469 tissues. This region contained CM-like stem cells, which were able to contribute to retinal
470 expansion by *de novo* generation of retinal progenitors.[89] Further exploration of the
471 mechanisms underlying CM-like stem cells will help advance ocular regenerative therapeutics.

472 **Retinal Organoids and disease modeling**

473 In recent years, retinal organoid models of various eye diseases have been created. These
 474 models can be either used for studying the underlying pathomechanisms as well as for therapeutic
 475 purposes. Table 1 summarizes some RO models of retinal diseases that have been developed thus far.
 476 However, some questions are arising regarding the further applicability of organoid models for
 477 disease modeling. Points to consider include whether the developmental “age” of the ROs
 478 corresponds to when the patient would get disease onset typically, or whether the culturing
 479 microenvironment exacerbates disease characteristics in organoid culture are concerns that need to be
 480 addressed in the upcoming studies. Modeling of the late-stage disease will be a particular challenge
 481 due to the immaturity of ROs even after long-term cell culture, the addition of stressors to induce
 482 aging phenotypes should be explored. Furthermore, ROs are still relatively naive structures that lack
 483 optic nerve, retinal vasculature, and microglia.

484

485 **Table 1**

Disease	Gene and mutation	Organoid features
	CEP290	
	[90,91]c.2991+1655A>G	Aberrant splicing, impaired ciliogenesis, reduced
LCA	homozygous mutation[90]	cilia incidence [90]
	Two patients heterozygous for IVS26+1655A>G and c.5668G>T mutations. One patient homozygous for IVS26 and 1655A>G [91]	Abnormal ciliogenesis, docked mother centriole and were only observed in optic cups derived from CEP290 LCA patients [91]

RPE65 [92] c.200T>G and c.430T>C	All patient lines could generate well-layered ROs, which contained rods and cones that had inner segments and rudimentary outer segments. However, no photoreceptor phenotype was observed. In patient RPE cells, which were generated simultaneously with ROs, a significant decrease in RPE65 expression was found. No differences in biological function, as measured by POS phagocytosis and VEGF secretion, was found in patient iPSC derived RPE compared to control.
AIPL1 [93] c.265 T > C homozygous mutation	Despite a reduction in both AIPL1 and PDE6B being found in patient ROs no retinal degeneration was detectable. Normal ultrastructural findings, expression of mature photoreceptor markers and similar gene expression profiles, except <i>NEUROD6</i> a transcription factor involved in amacrine cell subtype specification, were found between control and AIPL1-LCA ROs.
RPGR [94] c.1685_1686delAT, c.2234_2235delGA, c.2403_2404delAG mutations	Significant defects in photoreceptors, including decreased photoreceptor cell number, cilia length, and expression of photoreceptor-related genes, were found between control and patient ROs.

RP

When the electrophysiological properties of patient rod-like cells were examined compared to controls they were found to have a reduction in hyperpolarization-activated potassium current. This along with expression data highlighted a deficit in HCN channels.

CRB1 [72]

Patient 1:

c.3122T > C homozygous;

Patient 2:

2983G>T and c.1892A>G;

Patient 3:

c.2843G>A and c.3122T>C

Three hiPSC lines derived from *CRB1* RP patients, when differentiated into ROs, showed a phenotype of disruptions at the outer limiting membrane (OLM), as demonstrated by ectopic photoreceptor nuclei above the OLM. The degenerative retinal phenotype of *CRB1* RP patient hiPSC derived ROs was similar to that previously found in mice expressing variant *CRB1*^{C249W} or lacking *CRB1*. [95,96]

USH2A [97]

c.8559-2A > G

and c.9127_9129delTCC

Significant defects were identified from an early stage in patient compared to control ROs including delayed retinal self-organization, abnormal retinal neuroepithelium differentiation, and defective retinal progenitor cell development. A reduced diameter and thickness of the retinal neuroepithelium was found along with an increase in expression of apoptosis related genes

in patient ROs. Additionally, a decrease in retinal cells including photoreceptors, Müller and amacrine cell were found in patient ROs. Other RO defects included aberrant basement membrane and tight junctions. Further gene ontology analysis identified differentially expressed gene enriched for categories involved in calcium signaling, retinal layer formation, dopaminergic synapse and vesical transport.

Autosomal-dominant RP	<p>PRPF31 [98]</p> <p>Three related RP type 11 patients with c.1115_1125del11 heterozygous mutation.</p> <p>One patient with severe RP with c.522_527+10del heterozygous mutation.</p>	<p>Progressive degenerative features were found in ROs with TEM showing patient photoreceptors had an increase in apoptotic nuclei and the presence of stress vacuoles compared with controls. Additionally, a significantly reduced response was found in patient ROs to the neurotransmitter GABA. Patient ROs also exhibited impaired pre-mRNA splicing and had an increase in differentially expressed genes in gene ontology categories relating to the actin cytoskeleton, ciliary membrane, primary cilium, photoreceptor inner and outer segments, axon terminals and phototransduction. In accordance</p>
------------------------------	---	--

with this defective photoreceptor cilia were found in patient ROs.

Late-onset RP	PDE6B [65]		Patient ROs before DD180 exhibited relatively
	c.694G>A	homozygous	normal retinal development as compared with
	mutation.		controls. However, patient ROs at DD230 were
			found to have defective rod cell migration.
			Furthermore, gene ontology analysis found an
			enrichment of gene implicated in G-protein-
			coupled receptor activity, G-protein-coupled
			receptor signaling pathway and calcium ion
			binding in patient ROs. Additionally, an increase
			in cGMP levels were found in patient ROs,
			which may have led to the impaired formation of
			synaptic connections and the decrease in
			photoreceptor cilia found in patient ROs.
X-linked	RP2 [99]		RP2 patient-derived ROs exhibit a spike in cell
retinitis	R120X nonsense mutation		death in the ONL at DD150, with a subsequent
pigmentosa	c.358C > T		thinning of the ONL detectable at DD180. The
(XLRP)			onset of cell death coincides with the timing of
			rod cell maturation and rhodopsin expression. In
			accordance with the thinning ONL, a reduction in
			the number of rhodopsin positive cells in the

		ONL was detected at DD180.
Glaucoma	OPTN [100] E50K missense mutation	Early stages of retinal differentiation in ROs were unaffected by the OPTN(EK50) mutation. However, at later stages of maturation, retinal ganglion cells from derived from patient iPSCs exhibited neurite retraction, increased excitability, dysfunctional autophagy, as marked LC3 accumulation, and an increase in apoptosis of the inner retinal organoid.
X-linked Juvenile Retinoschisis (XLRS)	RS1 [101] Patient 1: c.625C>T Patient 2: c.488G>A	Retinal splitting, outer-segment defects, abnormal paxillin turnover, defective retinoschisin production, impaired ER-Golgi transportation, defective photoreceptor connecting cilia, and altered expression of retinopathy-associated genes including IQCB1 and OPA1, which are associated with LCA and autosomal dominant optic atrophy, respectively).
Retinoblastoma	RB1 [103] RB1-null mutations[103]	RB1 was found to be abundant in retinal progenitor cells and become downregulate during maturation of ROs. Loss of RB1, in RB1-null

ROs, promoted S-phase entry, lead to an increase in apoptosis and caused a reduction in the number of photoreceptors, bipolar, and ganglion cells. However, loss of RB1 was not sufficient to induce retinoblastoma formation in ROs.

486

487 LCA, Leber congenital amaurosis; CEP290, *centrosomal* protein 29; RP, retinitis pigmentosa;
 488 VEGF, vascular endothelial growth factor; AIPL1, Aryl hydrocarbon receptor-interacting
 489 protein-like 1; OS, outer segment; RO, retinal organoid; RPE, retinal pigment epithelium; RPC,
 490 retinal progenitor cell; cGMP, Cyclic guanosine monophosphate; ONL, outer nuclear layer;
 491 GPR161, G-protein-coupled receptor; OLM, outer limiting membrane; GFAP, Glial fibrillary
 492 acidic protein; OPTN, optineurin; NEUROD6, neuronal differentiation 6; *PDE6B*,
 493 Phosphodiesterase 6B; *IQCB1*, IQ Motif Containing B1; ERG, electroretinography; BM,
 494 basement membrane; HCN, hyperpolarization-activated cyclic nucleotide-gated; DD,
 495 differentiation day.

496

497 *ROs and therapeutics*

498 *Application to drug studies*

499 For drug studies, human RO technology promises to be a more realistic model of human
 500 development and disease than animal and 2-dimensional cell culture models [104,105]. RO models
 501 can be used to evaluate targeted therapy and drug toxicity in the pre-clinical drug development stage
 502 [106]. In what follows, we discuss two examples of RO-based drug studies. First, a model of
 503 advanced retinoblastoma tumor organoids (resembling retinal tumors and seeds) created by
 504 Saengwimol et al. was used to assess cell cycle arrest in response to drugs and their genotoxic effects.
 505 The model was used to compare the outcome of single drugs and their combinations. In the first step,
 506 they evaluated whether the result of this model will be comparable to clinical outcomes. Drugs
 507 commonly used in intravitreal chemotherapy, including melphalan, topotecan, and methotrexate were

508 used with various concentrations and 24-72(h) exposure times. Low dose melphalan (8 and 16 μ M)
509 with prolonged exposure time showed a similar effect to the high dose of melphalan (32 μ M) with
510 short exposure time, leading to induced S-phase arrest and reduced G2/M-phase. Topotecan (11 μ M)
511 efficiently reduced the number of tumor cells in G0/G1 and G2/M phases. Methotrexate showed the
512 least anticancer effectiveness. Methotrexate reduced the G0/G1-phase cells and increased cell death
513 in the sub-G1 phase, however, S and G2/M phases were activated. The results were comparable to
514 clinical results indicating the translatability of RO data. As topotecan and melphalan showed similar
515 effects, one may ask whether their combination will be a desired therapeutic strategy. Therefore, the
516 researchers took a second step to analyze targeted therapy and the genotoxicity of a combination of
517 topotecan (11 μ M) and melphalan (16 μ M), which was challenging to perform in clinics. The
518 combination not only had a profound influence on subretinal seeds or recurrent retinal tumors but
519 also targeted proliferative tumor cones effectively [102]. However, a combination of melphalan and
520 topotecan was more genotoxic than melphalan alone. This study thus shows the power of the RO
521 model in addressing therapeutic challenges.

522 In another study, Ito et al. used miPSC-derived ROs as a model for reproducing photoreceptor
523 degeneration treated by 4-hydroxytamoxifen (4-OHT) and diethylstilbestrol (DES) individually that
524 induces acute cell death. Additionally, they established a fluorescent live-cell imaging system in
525 order to evaluate their induced damage model. Those side effects were already confirmed in the
526 mouse retinal explant experiment. Therefore, ROs can recapitulate the drug side effects. They also
527 analyzed the protective effect of vitamin E (400 μ M) and Lutein (200 nM) as ophthalmic supplements
528 for treating the photoreceptor degeneration. The result showed the superior efficacy of vitamin E
529 compared to Lutein in suppressing oxidative and endoplasmic reticulum (ER) stress-related gene
530 [107]. Overall, ROs have been used in several proof-of-concept drug studies with promising results.

531 Nevertheless, there are several shortcomings, such as the lack of vascularization and immune cells.
532 Thus, current RO models cannot be used in drug studies such as screening of neuroprotective drug
533 development for retinopathy, where incorporation of inflammatory cells is essential [105].

534

535 *Application to Transplantation therapy*

536 Pluripotent stem cells can be used to provide a potentially unlimited supply of retinal
537 specific cell types. Retinal organoids derived from hESCs and hiPSCs can serve as a cellular
538 source for transplantation purposes, either as a retinal cell suspension or an organized retinal
539 sheet [108–111]. Most studies typically focus on the use of ROs as a source for rod and cone
540 photoreceptors, but they have also been used as a source for retinal ganglion cells and Müller
541 glial cells [62,109–113].

542 In 2016 a string of studies highlighted the need for reevaluation of previous
543 photoreceptor donor transplantation studies due to cytoplasmic material transfer between donor
544 and host cells [114–116]. These studies stressed that the propensity for transplanted donor
545 photoreceptors to integrate and provide functionality was more limited than initially thought,
546 with many of the observed functional benefits likely coming from the donor-host transfer of
547 phototransduction proteins [117,118]. The material transfer represents a novel therapeutic
548 strategy for the rescue of diseased retinal cells [76,119]. However, for the evaluation of current
549 photoreceptor transplantation experiments, the use of late-stage disease models in which the
550 majority of photoreceptor cells are lost may be preferable for the assessment of cell integration
551 and functional rescue. Nonetheless, the cell transplantation approach adopted, either cell
552 suspension or cell sheet, may reflect the disease stage needing to be treated. In milder
553 degenerative stages, donor cell suspensions may be advantageous. This is due to the preexisting

554 architecture in which the donor cells can integrate into and support the remaining host
555 photoreceptors. However, at later stages of degeneration, where few or no photoreceptors
556 remain, retinal sheets may be more optimal at surviving and forming synaptic connections with
557 the remaining inner retina.

558 Both photoreceptor cell suspensions and retinal sheets derived from ROs have been
559 explored for the treatment of late-stage models of retinal disease in which nearly all host
560 photoreceptors have already degenerated [62,108–110,120]. As an example, McLelland et al.
561 used hESC-derived ROs as a source of healthy retinal tissue to rescue an immunodeficient late-
562 stage retinal degenerative rat model. They found that the transplanted RO-derived retinal sheets
563 went under differentiation and integration, leading to an improvement in visual function, despite
564 the degenerative microenvironment. Analysis of the transplanted retinal sheets showed the
565 presence of rod and cone photoreceptors with putative outer segments, bipolar cells, Müller glial
566 cells, amacrine cells, and horizontal cells, which were all derived from the transplant. The
567 presence of increased immunoreactivity for synaptophysin near the transplanted cells compared
568 to areas further away from the transplant was suggestive of potential synaptic connectivity
569 between the host and transplanted cells [109]. While the presence of transplanted matured
570 photoreceptors with potential synaptic connectivity is extremely promising, the evaluation of
571 tangible functional rescue in degenerative models is still limited. As an example, the
572 immunodeficient rat model used both by McLelland et al. and Tu et al. were found to still have
573 light-responsive patches at 10 months of age, making it difficult to conclusively discriminate
574 graft-originated responses from the remaining host activity [109,120]. This highlights the need
575 for careful consideration when choosing which degenerative models to use for such experiments
576 and also highlights the need to confirm functionality using numerous approaches.

577 The CRISPR/Cas9, a technique has been used to correct mutations in patient iPSC lines
578 leading to the amelioration, when differentiated, of the RO phenotype compared to ROs derived
579 from the uncorrected patient line. This has been successfully studied on RO models of RP and
580 XLRs.[94,98,101] Patient corrected stem cell could be utilized as a source for autologous cell
581 transplantation for the treatment of retinal dystrophies. Lastly, during RO differentiation, there is
582 a concomitant generation of RPE. Dissected RPE spheroids from ROs or RPE spheroids
583 generated from the remaining cell culture after RO sorting can be used to generate RPE
584 monolayers or could be dissected to form RPE sheets [121]. Transplantation of RPE is a
585 promising strategy for treating advanced stages of eye disease such as RP, AMD, and Stargardt
586 disease (STGD1) in which significant RPE loss is found [122–124].

587

588 *Application to Gene therapy*

589 Adeno-associated virus (AAV) is a small, nonenveloped, replication-deficient, single-
590 stranded DNA parvovirus belonging to the genus Dependovirus. AAVs can be commandeered as
591 a delivery vector for gene augmentation, currently the therapeutic strategy of choice for targeting
592 hereditary retinal diseases [76,125]. Many studies have been performed using different
593 promoter/serotype combinations to assess cell tropism and transduction efficiency of AAVs in
594 ROs, with photoreceptors and radial glial progenitors/Müller glial cells being transduced
595 [60,72,99,126–128]. Here, we provide two recent examples of AAV-mediated gene delivery in
596 ROs.

597 Lane et al. used AAV2/5 to deliver the RP2 gene to photoreceptors in an organoid model
598 of X-linked retinitis pigmentosa (XLRP). RP2 patient-derived ROs exhibit a spike in cell death
599 in the ONL at differentiation day (DD)150, with a subsequent thinning of the ONL detectable at

600 DD180. The onset of cell death coincides with the timing of rod cell maturation and rhodopsin
601 expression. In accordance with the thinning ONL, a reduction in the number of rhodopsin
602 positive cells in the ONL was detected at DD180. After AAV2/5.CAGp.RP2 gene therapy, an
603 amelioration of this degenerative phenotype was observed, as marked by a reduction in ONL
604 thinning and restoration of rhodopsin expression.[99] This study highlights that the therapeutic
605 potential of AAV-mediated delivery of RP2 should be further explored as a treatment for XLRP.

606 The implementation of AAVs to deliver larger retinal genes is impeded by their limited
607 cargo capacity of approximately 5 kb of DNA. Recently, Tornabene et al. used split inteins to
608 mediate protein trans-splicing in human ROs. They found that multiple, AAV delivered, split
609 intein-flanked polypeptides could be reconstituted to form large full-length proteins in mouse,
610 pig, and human photoreceptors. Importantly, they were able to develop AAV-*ABCA4* and AAV-
611 *CEP290* intein vectors to improve the retinal phenotype found in STGD1 and LCA type 10
612 (LCA10) mouse models, respectively. Additionally, they were able to find expression of *ABCA4*
613 in STGD1 patient-derived ROs after administration of AAV2/2-GRK1-*ABCA4* intein vectors.

614 Patient-derived ROs are a promising alternative to animal models for the testing of AAV-
615 mediated gene augmentation strategies. However, the variability in AAV transduction
616 efficiencies in ROs needs to be addressed [60,72,99,126–128]. Variations in transduction
617 efficiencies may be due to the methodology used to generate ROs, promoter choice, viral titre,
618 vector tropism, transgene detection method, timepoint of viral vector administration to RO, and
619 the number of days post-administration before RO collection and analysis.[99] Particularly, the
620 developmental timepoint specific bioavailability of receptors for AAV uptake may be a critical
621 consideration for efficient transduction of RO cell types and therefore AAV vector choice

622 [72,128]. Additionally, lentivirus is also capable of efficiently transducing photoreceptors in ROs
623 and is an alternative delivery strategy to be further explored [85,106].

624

625 **Retina chips**

626 Numerous physiological processes and disease progressions in the retina involve the
627 presence of cells and structures from multiple developmental origins. For instance, blood vessels
628 and immune cells, originating from outside the retinal lineage, play a critical role in the onset and
629 progression of diabetic retinopathy and the wet form of age-related macular degeneration (wet-
630 AMD) [129]. Retinal organoids as previously described can reflect a majority of the cell types
631 and architecture of the retina, but cannot faithfully recreate several important disease-relevant
632 structures such as the inner and outer blood-retina barriers (iBRB and oBRB).

633 Organ chips are particularly well suited to model these tissue barriers since they enable a
634 multilayered alignment of cells as well as a blood stream-like perfusion [130]. Thus, a prime
635 application for retina-based chips is the modeling of the blood-retina-barriers (BRB), in
636 particular, the outer BRB (oBRB), formed by retinal pigmented epithelial cells (RPE), and the
637 adjacent choroidal microvascular network formed by microcapillary endothelial cells [131]. The
638 simplest oBRB on-chip arrangement poses a two-channeled organ chip where RPE and
639 endothelial cells are seeded on opposite sides of a porous membrane. Subsequent perfusion by a
640 medium pump is then used to recreate a microvascular blood flow.

641 In 2017, Chen et al. applied this concept using the RPE cell line ARPE19 and human
642 umbilical vein endothelial cells (HUVEC) [132]. The chip was used to study the migration of
643 HUVEC cells into the RPE compartment in normal, hypoxic, and hypoglycemic conditions. In

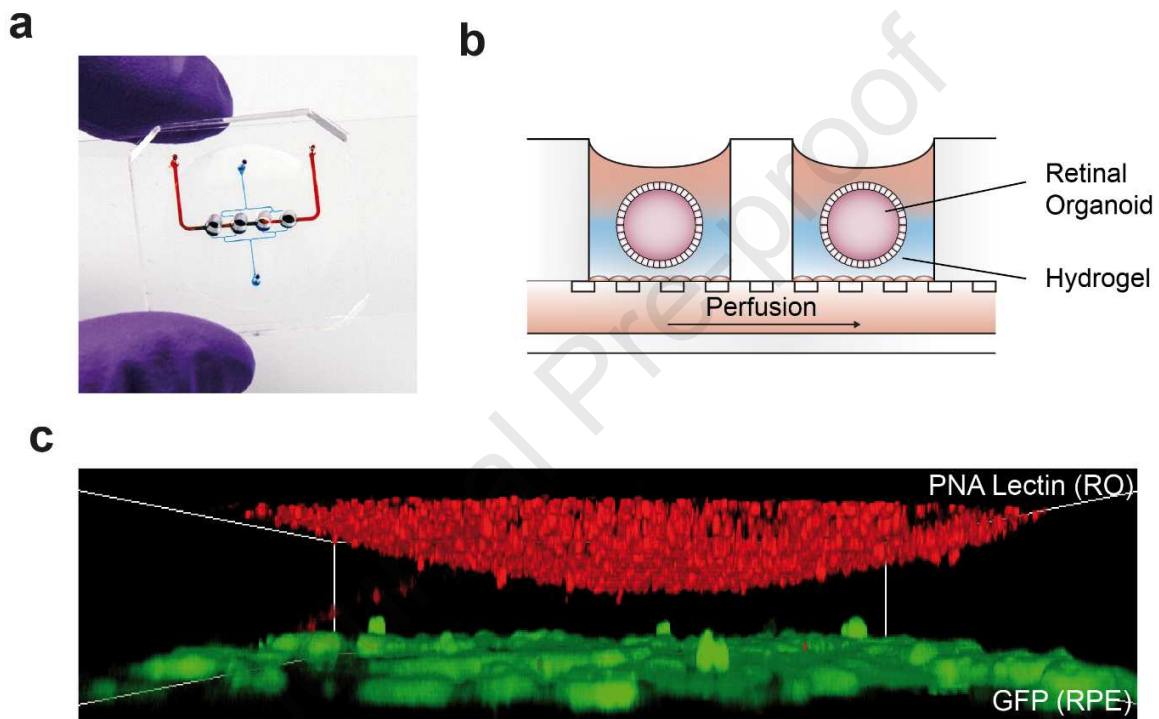
644 all conditions, a decline of RPE cell number was observed, whereas the HUVEC cells migrated
645 through the membrane towards the RPE layer.

646 In the same year, Chung et al. presented a slightly different chip concept replacing the
647 porous membrane by a fibrin hydrogel gap [133]. To mimic the three-dimensional choroidal
648 vascular network, endothelial cells mixed with the fibrin gel were seeded in a channel below the
649 fibrin gap. RPE (ARPE19) cells were seeded on the gel wall above in a separate chamber. Upon
650 stimulation with the angiogenic growth factor VEGF, the choroidal endothelial cells infiltrated
651 the fibrin gap and the RPE layer, recapitulating the pathogenic processes occurring in wet-AMD.
652 Subsequent treatment with the anti-VEGF antibody bevacizumab, a widely used wet-AMD drug,
653 could prevent the vessels spreading, emphasizing that blood-retina barrier chips can not only
654 reproduce pathophysiological processes but also reproduce therapeutic approaches.

655 The next generation of chip systems was then aiming to not simply reproduce the outer
656 barrier function of the retina but also to integrate the neural retina and the blood vessels barriers
657 within the retina (iBRB). Following that idea, Yeste et al. used a multilayered chip design which
658 was separated by several permeable membranes [134]. Besides the RPE (ARPE19) component,
659 representing the oBRB and primary human retinal endothelial cells, representing the iBRB, they
660 integrated a neuroblastoma cell line (SH-SY5Y), mimicking the neural part of the retina. Via the
661 integration of a transepithelial electrical resistance measurement (TEER) system, they then
662 validated the barrier functionalities of the iBRB and oBRB.

663 The retina chip introduced in 2019 by Achberger et al. aimed for modeling the oBRB
664 together with the neural retina [135] (Fig. 4). By combining hiPSC-ROs with adherently cultured
665 hiPSC-derived retinal pigment epithelium (RPE), they combined all major retinal cell types on
666 one platform. The benefits of this chip were to have a sub-RPE choroidal-like perfusion through

667 the microfluidic channels of the chip, the recreate of the oBRB using iPSC-derived RPE and to
 668 connect the photoreceptors (PRC) of the ROs with their direct neighbor cell type *in vivo*, the
 669 RPE. This close PRC-RPE proximity led to an increase of photoreceptor outer segment number
 670 after 7 days of co-culture as well as active phagocytosis of photoreceptor segments by the
 671 hiPSC- RPE.



672
 673 *Figure 4: The engineered retina chip model. (a) Image of the chip. Medium channels are colored*
 674 *with dyes for visualization. (b) A schematic concept of the retina chip. (c) A 3d reconstruction of*
 675 *a retinal organoid labeled by the photoreceptor surface marker PNA Lectin (red) and GFP-*
 676 *labelled hiPSC-derived RPE cells in the retina chip. Adapted from Achberger et al., 2019, CC*
 677 *BY 4.0 [135].*

678

679 **Application to Drug studies**

680 As retina chips are able to mimic physiological processes and barriers in the retina, they
681 are of high interest for the preclinical evaluation of drug effects [135,136]. In a proof-of-
682 principle study, the retina chip from Achberger et al. was supplemented with chloroquine (anti-
683 malaria drug) and gentamicin (antibiotic drug), which have both a detrimental effect on the
684 retina. The retinopathic and toxic side effects observed *in vivo* could be reproduced, shown by
685 staining cell death by propidium iodide (PI) and the lysosomal marker LAMP2. High doses of
686 chloroquine (80mg/ml) resulted in significant PI staining and an increase in LAMP2, reflecting
687 the lysosomal dysfunction observed *in vivo* [137]. The toxicity of Gentamicin in the retina chip
688 was dependent upon the presence of RPE. A decrease in toxicity was found in the presence of
689 RPE indicating that these cells might act as a barrier that protects the retinal organoids from
690 gentamicin toxicity.

691 Retina chips have also been used to develop and test intraocular tamponades. Silicone oil
692 (SO) is commonly used as intraocular tamponade in different eye diseases such as retinal
693 detachment and giant retinal tears [138,139]. Chan et al. analyzed the formation of SO droplets
694 in a microfluidic chip designed with a retinal ganglion cell line to mimic the eye cavity [140]. In
695 this study, the researchers could measure the size as well as the number of SO droplets and
696 reproduced SO-aqueous interface.

697

698 Application to cell (transplantation) therapy

699 The efficiency of therapies to replace dysfunctional photoreceptors by RPCs is highly
700 based on the migration of cells collectively and in the correct direction [141].

701 Mirsha et al. used a microfluidic model of the retina to study the effect of human and mouse eye
702 geometries on retinal cell migration [142]. Using computational models and experiments, they
703 found that a concentration gradient of stromal cell-derived factor 1 (SDF-1) was formed and
704 played as a force for chemotaxis; in the high concentration of SDF-1, cells migrated toward
705 higher concentrations of it while in low concentrations they did not move. Thakur et al. studied
706 the adhesive and displacement dynamics of RPCs to check if the biomaterial used in
707 transplantation can enhance and coordinate cell migrations [143]. Using a μ Lane, they found that
708 cell-cell interactions are dominant when hyaluronic acid or laminin was used as a transplantation
709 matrix while high cell-matrix interactions in fibronectin result in cell monolayer formation.
710 These findings emphasize the importance of substrate nature in enhancing the efficiency of
711 migration and consequently in the success of transplantation. The same concept was investigated
712 further using *Drosophila melanogaster* as a model organism combined with microfluidics by
713 Pena et al. [144]. A novel electro-chemotactic study of the migratory behavior of RPCs was
714 conducted by Mishra et al.[145]. By fabricating a galvano-microfluidic system, they were able to
715 establish tunable superimposed electric fields to study its effects on cellular motility.
716 Interestingly, they found that by using a combination of electric field and SDF-1 concentration
717 gradient, not only the migration distance can be increased about three times, but also the
718 directionality will be enhanced. By performing bioinformatics analysis, it was found that the
719 reason was the down-regulation of adhesion proteins simultaneously with the up-regulation of
720 cytoskeletal regulatory proteins. These studies pave the way for developing more advanced RC
721 models to simulate post-transplantation remodeling.

722

723 **Lens**

724 The initial steps for growing lens organoids or lentoid bodies (LBs) were made in the
725 1970s [146]. Three decades later, Yang and colleagues were the first to derive lens progenitor
726 cells and LBs from hESCs.[147] They deployed a three-stage culturing system via sequential
727 inhibition and activation of FGF, TGF- β , and Wnt signaling pathways. They could successfully
728 culture a large number of LBs with this technique. Bone Morphogenetic Protein (BMP) signaling
729 inhibition by noggin triggered cells towards neuroectodermal fate. Also, the role of FGF2 was
730 found to be necessary for lentoid formation. Their model was limited in a few aspects. For
731 example, terminal differentiation of the lens fibers was properly initiated but not completely
732 executed, marked by the lower amounts of β - and γ -crystallins in LBs compared to the human
733 lens but with comparable amounts in the initiation period. The LBs also tended to dissociate
734 from their support from day 35 of culture. The use of 3D matrices containing laminin, collagen,
735 and fibronectin, have allowed differentiation of LBs past day 35. Lacking light focusing ability
736 was also one of the limitations of their model. Fu et al. used hiPSCs and induced them to lens
737 progenitor cells and LBs by using a “fried egg” differentiation method. The cells in this method
738 have a fried egg appearance at a time during differentiation, with the yolk serving as E-cadherin⁺
739 differentiating cells (D-cells) which eventually form the LBs, and the egg white serving as E-
740 cadherin⁻ supporting cells (S cells) [148]. By using the same method of differentiation, they
741 studied the autophagic activity in LBs derived from human iPSCs and ESCs. Their model can be
742 used to investigate abnormalities in organelle degradation to form an organelle free zone (OFZ)
743 during lens development [149]. Having an OFZ is crucial for the proper homeostasis of the lens,
744 leading to cataract formation if disrupted. LBs have been successfully derived from cataract
745 patient iPSCs [150]. The LBs can be used for studying various causes of cataracts, including
746 congenital cataracts and age-related cataracts (ARC) [151,152]. For modeling ARC, it has been

747 found that LBs spontaneously become cloudy after a prolonged time in culture, which is
748 accompanied by protein aggregation. The use of hydrogen peroxide accelerates this process. This
749 model system may be a suitable ARC disease model for understanding the role of oxidative
750 stress in cataractogenesis [152].

751 Murphy et al. developed an alternative differentiation methodology that generated LBs
752 which contained minimal non-lens cells [153]. In contrast to the previous LB models, their
753 model yielded more spherical mini-lenses with a biconvex appearance and with more light
754 focusing ability. They could purify their cells by performing Magnetic-activated cell sorting
755 (MACS) to select cells expressing receptor tyrosine kinase-like orphan receptor 1 (ROR1),
756 acting as a potential lens epithelial cell (LEC) purification agent. Their system is ROR1⁺ micro-
757 lens system. They also suggested that their model can be used to study posterior capsule
758 opacification (PCO), which is considered the most common complication of cataract surgery.
759 Their model can effectively serve to understand the underlying mechanisms behind cataract risk
760 factors, including age, diabetics, ultraviolet (UV) light, radiation, smoking, drug-induced,
761 medications. The protein aggregates causing cataract or other particles causing light-scattering in
762 the lens can be tested under high-throughput screening (HTS) conditions also for therapeutic
763 targets. Most of the transcriptomic profile is expressed in LBs. Ali et al. compared the LBs
764 derived from hESCs and peripheral blood mononuclear cell (pBMc)-originated hiPSCs in terms
765 of their transcriptomic profile. They found that almost 70% of the total human protein-coding
766 transcriptome is expressed in LBs. The hESCs and hiPSCs shared more than 96% in the
767 similarity of transcriptome gene expression. However, they realized that the hiPSCs yield more
768 differential gene expressions, including 416 down- and 291 up-regulated genes [154].

769

770 **Discussion and Conclusion**

771 Engineered organoids and organ chips will inevitably change the way we do *in vitro*
772 eye research in the future. In particular, they provide us with the possibility to study
773 individualized differences in disease manifestations [155]. Despite recent advances, there are
774 some drawbacks and challenges that need to be addressed [156]. Technical variability is a major
775 issue in organoid systems, as such standardized protocols are needed to avoid inconsistencies
776 between results reported by different laboratories. Similarly, the use of well-characterized
777 commercially available pluripotent stem cell lines would aid in the interpretation of results
778 between labs. Lack of vasculature is preventing the study of vascular diseases like diabetes and
779 high-risk corneal transplantation. Another important issue is the difficulty of modeling
780 interactions between different eye tissues. Organ chips may help in this regard; however, this in
781 turn comes with its own shortcomings [157]. Cornea and retina chips are powerful *in vitro* tools
782 to study drug effects, therapeutic approaches, and disease-relevant questions, but the current
783 chips, however, are still minimalistic. Future developments could make these chips even more
784 complex, reflecting, and recreating an increasing number of functional and anatomical cues of
785 the human eye, which may undergo critical changes in aging and disease[158][159].

786 We expect that future use of organoids and organ chips will lead to a surge of new
787 research directions. Viral diseases and microbiome analysis are two areas where such approaches
788 may impact ophthalmology. It is often hard to model human viral diseases in animals due to the
789 specificities of virus-host interactions. Organ chips and organoids have recently been introduced
790 to the field of virology [160]. Over the past decades, a major advance in medicine has been the
791 recognition of the critical role of the microbiome in health and disease. The organ chip
792 technology provides a way to study direct interaction between the microbiome and the different

793 kinds of tissues outside the human body. For example, the intestine chip model provided a
794 discovery tool to study the diverse microbiome-related therapeutics [161]. The significance of
795 the ocular microbiome for ocular surface diseases such as DED has recently been recognized
796 [162]. In the future, ocular microbiome chip technology will expectedly emerge as a new concept
797 and an interdisciplinary approach in the pathobiology and clinical management of ocular surface
798 diseases and beyond [162].

799 Finally, the full potential of *in vitro* modeling will only be realized if relevant
800 measurement approaches are developed to extract biochemical and physical data from the
801 engineered models. Advances in omics technology, in particular, are crucial in this regard. For
802 example, metabolomics has only recently been introduced to the field of ocular surface
803 diseases[163]. Application of these techniques to the human eye and the engineered models
804 require protocols that allow for handling small volumes and a small number of cells. Current
805 research in analytical biosciences in parallel to the bio-inspired engineering methodology
806 promises great potential for organoids and organ chips in clinical translational research.

807 Lastly, organoids and organ chip technologies will allow for the testing of new
808 therapeutic paradigms. For example, precision metabolome reprogramming was recently
809 highlighted as a promising non-gene-specific therapeutic avenue for inherited retinal dystrophies
810 which would be of interest to explore in a complex retina chip format which also contained
811 microglia in addition to RPE and retina.[164]

812

813 **Financial support**

814 PMJQ is funded by the Curing Retinal Blindness Foundation (CRBF) and The Knights Templar
815 Eye Foundation (KTEF). S.L. acknowledges DFG (DFG LI 2044/4-1 and DFG LI 2044/5-1 for
816 support.

817

818 **Disclosure/conflict of interest**

819 None

820

821 **Acknowledgments**

822 PMJQ would like to thank his team members at JCVC. Graphical abstract 'Created with
823 BioRender'.

824

825 **References**

826

827 [1] Graw J. Eye development. *Curr Top Dev Biol* 2010;90:343–86.

828 [https://doi.org/10.1016/S0070-2153\(10\)90010-0](https://doi.org/10.1016/S0070-2153(10)90010-0).

829 [2] Takahashi M, Haruta M. Derivation and characterization of lentoid bodies and retinal

830 pigment epithelial cells from monkey embryonic stem cells in vitro. *Methods Mol Biol*

831 2006;330:417–29. <https://doi.org/10.1385/1-59745-036-7:417>.

832 [3] Rountree CM, Troy JB, Saggere L. Methodology for biomimetic chemical

833 neuromodulation of rat retinas with the neurotransmitter glutamate in vitro. *J Vis Exp*

834 2017;2017:1–13. <https://doi.org/10.3791/56645>.

835 [4] Elliott NT, Yuan F. A Review of Three-Dimensional In Vitro Models for Drug Discovery

836 and Transport Studies. *J Pharmaceutical Sci* 2011;100:59–73. <https://doi.org/10.1002/jps>.

- 837 [5] Meyer JS, Shearer RL, Capowski EE, Wright LS, Wallace K a, McMillan EL, et al.
838 Modeling early retinal development with human embryonic and induced pluripotent stem
839 cells. *Proc Natl Acad Sci U S A* 2009;106:16698–703.
840 <https://doi.org/10.1073/pnas.0905245106>.
- 841 [6] Quinn PM, Alves CH, Klooster J, Wijnholds J. CRB2 in immature photoreceptors
842 determines the superior-inferior symmetry of the developing retina to maintain retinal
843 structure and function. *Hum Mol Genet* 2018;27:3137–53.
844 <https://doi.org/10.1093/hmg/ddy194>.
- 845 [7] Quinn PM, Mulder AA, Henrique Alves C, Desrosiers M, de Vries SI, Klooster J, et al.
846 Loss of CRB2 in Müller glial cells modifies a CRB1-associated retinitis pigmentosa
847 phenotype into a Leber congenital amaurosis phenotype. *Hum Mol Genet* 2019;28:105–
848 23. <https://doi.org/10.1093/hmg/ddy337>.
- 849 [8] Pellissier LP, Quinn PM, Alves CH, Vos RM, Klooster J, Flannery JG, et al. Gene therapy
850 into photoreceptors and Müller glial cells restores retinal structure and function in CRB1
851 retinitis pigmentosa mouse models. *Hum Mol Genet* 2015;24:3104–18.
852 <https://doi.org/10.1093/hmg/ddv062>.
- 853 [9] Tsai YT, Wu WH, Lee TT, Wu WP, Xu CL, Park KS, et al. Clustered Regularly
854 Interspaced Short Palindromic Repeats-Based Genome Surgery for the Treatment of
855 Autosomal Dominant Retinitis Pigmentosa. *Ophthalmology* 2018;125:1421–30.
856 <https://doi.org/10.1016/j.ophtha.2018.04.001>.
- 857 [10] Boye SE, Alexander JJ, Boye SL, Witherspoon CD, Sandefer KJ, Conlon TJ, et al. The
858 human rhodopsin kinase promoter in an AAV5 vector confers rod- and cone-specific
859 expression in the primate retina. *Hum Gene Ther* 2012;23:1101–15.

- 860 <https://doi.org/10.1089/hum.2012.125>.
- 861 [11] Vandenberghe LH, Bell P, Maguire AM, Xiao R, Hopkins TB, Grant R, et al. AAV9
862 targets cone photoreceptors in the nonhuman primate retina. *PLoS One* 2013;8:e53463.
863 <https://doi.org/10.1371/journal.pone.0053463>.
- 864 [12] Lin S, Lin Y, Nery JR, Urich MA, Breschi A, Davis CA, et al. Comparison of the
865 transcriptional landscapes between human and mouse tissues. *Proc Natl Acad Sci U S A*
866 2014;111:17224–9. <https://doi.org/10.1073/pnas.1413624111>.
- 867 [13] Eiraku M, Takata N, Ishibashi H, Kawada M, Sakakura E, Okuda S, et al. Self-organizing
868 optic-cup morphogenesis in three-dimensional culture. *Nature* 2011;472:51–6.
869 <https://doi.org/10.1038/nature09941>.
- 870 [14] Seo J, Byun WY, Alisafaei F, Georgescu A, Yi YS, Massaro-Giordano M, et al.
871 Multiscale reverse engineering of the human ocular surface. *Nat Med* 2019;25:1310–8.
872 <https://doi.org/10.1038/s41591-019-0531-2>.
- 873 [15] Clevers H. Modeling Development and Disease with Organoids. *Cell* 2016;165:1586–97.
874 <https://doi.org/10.1016/j.cell.2016.05.082>.
- 875 [16] Xinaris C, Briza V, Remuzzi G. Organoid Models and Applications in Biomedical
876 Research. *Nephron* 2015;130:191–9. <https://doi.org/10.1159/000433566>.
- 877 [17] Minami Y, Sugihara H, Oono S. Reconstruction of cornea in three-dimensional collagen
878 gel matrix culture. *Invest Ophthalmol Vis Sci* 1993;34:2316–24.
- 879 [18] Germain L, Auger FA, Grandbois E, Guignard R, Giasson M, Boisjoly H, et al.
880 Reconstructed human cornea produced in vitro by tissue engineering. *Pathobiology*
881 1999;67:140–7.
- 882 [19] Griffith M, Osborne R, Munger R, Xiong X, Doillon CJ, Laycock NLC, et al. Functional

- 883 Human Corneal Equivalent Constructed from Cell Lines. *Science* (80-) 1999;286:2169–
 884 72.
- 885 [20] Lancaster M a., Knoblich J a. Organogenesis in a dish: modeling development and disease
 886 using organoid technologies. *Science* 2014;345:1247125.
 887 <https://doi.org/10.1126/science.1247125>.
- 888 [21] Chakrabarty K, Shetty R, Ghosh A. Corneal cell therapy: with iPSCs, it is no more a far-
 889 sight. *Stem Cell Res Ther* 2018;9:1–15. <https://doi.org/10.1186/s13287-018-1036-5>.
- 890 [22] Zhang C, Du L, Pang K, Wu X. Differentiation of human embryonic stem cells into
 891 corneal epithelial progenitor cells under defined conditions. *PLoS One* 2017;12:1–17.
 892 <https://doi.org/10.1371/journal.pone.0183303>.
- 893 [23] Hongisto H, Vattulainen M, Ilmarinen T, Mikhailova A, Skottman H. Efficient and
 894 scalable directed differentiation of clinically compatible corneal limbal epithelial stem
 895 cells from human pluripotent stem cells. *J Vis Exp* 2018;2018:1–9.
 896 <https://doi.org/10.3791/58279>.
- 897 [24] Erhani J, Aberdam D, Larghero J, Vanneaux V. Pluripotent Stem Cells and Other
 898 Innovative Strategies for the Treatment of Ocular Surface Diseases. *Stem Cell Rev*
 899 *Reports* 2016;12:171–8. <https://doi.org/10.1007/s12015-016-9643-y>.
- 900 [25] Foster JW, Wahlin K, Adams SM, Birk DE, Zack DJ, Chakravarti S. Cornea organoids
 901 from human induced pluripotent stem cells. *Sci Rep* 2017;7:1–8.
 902 <https://doi.org/10.1038/srep41286>.
- 903 [26] Susaimanickam PJ, Maddileti S, Kumar Pulimamidi V, Boyinpally SR, Naik RR, Naik
 904 MN, et al. Generating minicorneal organoids from human induced pluripotent stem cells.
 905 *Dev* 2017;144:2338–51. <https://doi.org/10.1242/dev.143040>.

- 906 [27] Puleo CM, McIntosh Ambrose W, Takezawa T, Elisseff J, Wang TH. Integration and
907 application of vitrified collagen in multilayered microfluidic devices for corneal
908 microtissue culture. *Lab Chip* 2009;9:3221–7. <https://doi.org/10.1039/b908332d>.
- 909 [28] Bennet D, Estlack Z, Reid T, Kim J. A microengineered human corneal epithelium-on-a-
910 chip for eye drops mass transport evaluation. *Lab Chip* 2018;18:1539–51.
911 <https://doi.org/10.1039/c8lc00158h>.
- 912 [29] Bai J, Fu H, Bazinet L, Birsner AE, D'amato RJ. A method for developing novel 3D
913 cornea-on-a-chip using primary murine corneal epithelial and endothelial cells. *Front*
914 *Pharmacol* 2020. <https://doi.org/10.3389/fphar.2020.00453>.
- 915 [30] Pispa J, Thesleff I. Mechanisms of ectodermal organogenesis. *Dev Biol* 2003;262:195–
916 205. [https://doi.org/10.1016/s0012-1606\(03\)00325-7](https://doi.org/10.1016/s0012-1606(03)00325-7).
- 917 [31] De Robertis EM. Spemann's organizer and the self-regulation of embryonic fields. *Mech*
918 *Dev* 2009;126:925–41. <https://doi.org/10.1016/j.mod.2009.08.004>.
- 919 [32] Nakao K, Morita R, Saji Y, Ishida K, Tomita Y, Ogawa M, et al. The development of a
920 bioengineered organ germ method. *Nat Methods* 2007;4:227–30.
921 <https://doi.org/10.1038/nmeth1012>.
- 922 [33] Ikeda E, Morita R, Nakao K, Ishida K, Nakamura T, Takano-Yamamoto T, et al. Fully
923 functional bioengineered tooth replacement as an organ replacement therapy. *Proc Natl*
924 *Acad Sci U S A* 2009;106:13475–80. <https://doi.org/10.1073/pnas.0902944106>.
- 925 [34] Oshima M, Mizuno M, Imamura A, Ogawa M, Yasukawa M, Yamazaki H, et al.
926 Functional tooth regeneration using a bioengineered tooth unit as a mature organ
927 replacement regenerative therapy. *PLoS One* 2011;6:e21531.
928 <https://doi.org/10.1371/journal.pone.0021531>.

- 929 [35] Toyoshima KE, Asakawa K, Ishibashi N, Toki H, Ogawa M, Hasegawa T, et al. Fully
 930 functional hair follicle regeneration through the rearrangement of stem cells and their
 931 niches. *Nat Commun* 2012;3:784. <https://doi.org/10.1038/ncomms1784>.
- 932 [36] Ogawa M, Oshima M, Imamura A, Sekine Y, Ishida K, Yamashita K, et al. Functional
 933 salivary gland regeneration by transplantation of a bioengineered organ germ. *Nat*
 934 *Commun* 2013;4:2498. <https://doi.org/10.1038/ncomms3498>.
- 935 [37] Hirayama M, Ogawa M, Oshima M, Sekine Y, Ishida K, Yamashita K, et al. Functional
 936 lacrimal gland regeneration by transplantation of a bioengineered organ germ. *Nat*
 937 *Commun* 2013;4:2497. <https://doi.org/10.1038/ncomms3497>.
- 938 [38] Eiraku M, Watanabe K, Matsuo-Takasaki M, Kawada M, Yonemura S, Matsumura M, et
 939 al. Self-organized formation of polarized cortical tissues from ESCs and its active
 940 manipulation by extrinsic signals. *Cell Stem Cell* 2008;3:519–32.
 941 <https://doi.org/10.1016/j.stem.2008.09.002>.
- 942 [39] Sato T, Vries RG, Snippert HJ, van de Wetering M, Barker N, Stange DE, et al. Single
 943 Lgr5 stem cells build crypt-villus structures in vitro without a mesenchymal niche. *Nature*
 944 2009;459:262–5. <https://doi.org/10.1038/nature07935>.
- 945 [40] Nakano T, Ando S, Takata N, Kawada M, Muguruma K, Sekiguchi K, et al. Self-
 946 formation of optic cups and storable stratified neural retina from human ESCs. *Cell Stem*
 947 *Cell* 2012;10:771–85. <https://doi.org/10.1016/j.stem.2012.05.009>.
- 948 [41] Antonica F, Kasprzyk DF, Opitz R, Iacovino M, Liao XH, Dumitrescu AM, et al.
 949 Generation of functional thyroid from embryonic stem cells. *Nature* 2012;491:66–71.
 950 <https://doi.org/10.1038/nature11525>.
- 951 [42] Dye BR, Hill DR, Ferguson MA, Tsai YH, Nagy MS, Dyal R, et al. In vitro generation of

- 952 human pluripotent stem cell derived lung organoids. *Elife* 2015;4.
953 <https://doi.org/10.7554/eLife.05098>.
- 954 [43] Spence JR, Mayhew CN, Rankin SA, Kuhar MF, Vallance JE, Tolle K, et al. Directed
955 differentiation of human pluripotent stem cells into intestinal tissue in vitro. *Nature*
956 2011;470:105–9. <https://doi.org/10.1038/nature09691>.
- 957 [44] Tanaka J, Ogawa M, Hojo H, Kawashima Y, Mabuchi Y, Hata K, et al. Generation of
958 orthotopically functional salivary gland from embryonic stem cells. *Nat Commun*
959 2018;9:4216. <https://doi.org/10.1038/s41467-018-06469-7>.
- 960 [45] Hirayama M, Ko SBH, Kawakita T, Akiyama T, Goparaju SK, Soma A, et al.
961 Identification of transcription factors that promote the differentiation of human pluripotent
962 stem cells into lacrimal gland epithelium-like cells. *NPJ Aging Mech Dis* 2017;3:1.
963 <https://doi.org/10.1038/s41514-016-0001-8>.
- 964 [46] Aakalu VK, Parameswaran S, Maienschein-Cline M, Bahroos N, Shah D, Ali M, et al.
965 Human Lacrimal Gland Gene Expression. *PLoS One* 2017;12:e0169346.
966 <https://doi.org/10.1371/journal.pone.0169346>.
- 967 [47] Gromova A, Voronov DA, Yoshida M, Thotakura S, Meech R, Dartt DA, et al. Lacrimal
968 Gland Repair Using Progenitor Cells. *Stem Cells Transl Med* 2017;6:88–98.
969 <https://doi.org/10.5966/sctm.2016-0191>.
- 970 [48] Hirayama M, Ogawa M, Oshima M, Sekine Y, Ishida K, Yamashita K, et al. Functional
971 lacrimal gland regeneration by transplantation of a bioengineered organ germ. *Nat*
972 *Commun* 2013. <https://doi.org/10.1038/ncomms3497>.
- 973 [49] Brinton M, Kossler AL, Patel ZM, Loudin J, Franke M, Ta CN, et al. Enhanced Tearing
974 by Electrical Stimulation of the Anterior Ethmoid Nerve. *Invest Ophthalmol Vis Sci*

- 975 2017;58:2341–8. <https://doi.org/10.1167/iovs.16-21362>.
- 976 [50] Spaniol K, Metzger M, Roth M, Greve B, Mertsch S, Geerling G, et al. Engineering of a
977 Secretory Active Three-Dimensional Lacrimal Gland Construct on the Basis of
978 Decellularized Lacrimal Gland Tissue. *Tissue Eng Part A* 2015;21:2605–17.
979 <https://doi.org/10.1089/ten.TEA.2014.0694>.
- 980 [51] Lin H, Sun G, He H, Botsford B, Li M, Elisseeff JH, et al. Three-Dimensional Culture of
981 Functional Adult Rabbit Lacrimal Gland Epithelial Cells on Decellularized Scaffold.
982 *Tissue Eng Part A* 2016;22:65–74. <https://doi.org/10.1089/ten.TEA.2015.0286>.
- 983 [52] Kobayashi S, Kawakita T, Kawashima M, Okada N, Mishima K, Saito I, et al.
984 Characterization of cultivated murine lacrimal gland epithelial cells. *Mol Vis*
985 2012;18:1271–7.
- 986 [53] Chung SH, Lee JH, Yoon JH, Lee HK, Seo KY. Multi-layered culture of primary human
987 conjunctival epithelial cells producing MUC5AC. *Exp Eye Res* 2007;85:226–33.
988 <https://doi.org/10.1016/j.exer.2007.04.005>.
- 989 [54] Schrader S, Kremling C, Klinger M, Laqua H, Geerling G. Cultivation of lacrimal gland
990 acinar cells in a microgravity environment. *Br J Ophthalmol* 2009;93:1121–5.
991 <https://doi.org/10.1136/bjo.2008.137927>.
- 992 [55] Schechter J, Stevenson D, Chang D, Chang N, Pidgeon M, Nakamura T, et al. Growth of
993 purified lacrimal acinar cells in Matrigel raft cultures. *Exp Eye Res* 2002;74:349–60.
994 <https://doi.org/10.1006/exer.2001.1158>.
- 995 [56] Selvam S, Thomas PB, Trousdale MD, Stevenson D, Schechter JE, Mircheff AK, et al.
996 Tissue-engineered tear secretory system: functional lacrimal gland acinar cells cultured on
997 matrix protein-coated substrata. *J Biomed Mater Res B Appl Biomater* 2007;80:192–200.

- 998 <https://doi.org/10.1002/jbm.b.30584>.
- 999 [57] Lu Q, Yin H, Grant MP, Elisseeff JH. An In Vitro Model for the Ocular Surface and Tear
1000 Film System. *Sci Rep* 2017;7:6163. <https://doi.org/10.1038/s41598-017-06369-8>.
- 1001 [58] Eiraku M, Sasai Y. Mouse embryonic stem cell culture for generation of three-
1002 dimensional retinal and cortical tissues. *Nat Protoc* 2012;7:69–79.
1003 <https://doi.org/10.1038/nprot.2011.429>.
- 1004 [59] Zhong X, Gutierrez C, Xue T, Hampton C, Vergara MN, Cao L-H, et al. Generation of
1005 three-dimensional retinal tissue with functional photoreceptors from human iPSCs. *Nat*
1006 *Commun* 2014;5:4047. <https://doi.org/10.1038/ncomms5047>.
- 1007 [60] Tso A, Ragi SD, Costa BLD, Li Y, Quinn PMJ. Molecular and therapeutic strategies for
1008 Retinitis Pigmentosa: Generation of Human iPSC-Derived Retinal Organoids for
1009 Assessment of AAV-Mediated Gene Delivery. . In: Walker JM, ed. *Methods Mol Biol*
1010 2020;In Press:2020.
- 1011 [61] Reichman S, Slembrouck A, Gagliardi G, Chaffiol A, Terray A, Nanteau C, et al.
1012 Generation of Storable Retinal Organoids and Retinal Pigmented Epithelium from
1013 Adherent Human iPS Cells in Xeno-Free and Feeder-Free Conditions. *Stem Cells*
1014 2017;35:1176–88. <https://doi.org/10.1002/stem.2586>.
- 1015 [62] Gonzalez-Cordero A, Kruczek K, Naeem A, Fernando M, Kloc M, Ribeiro J, et al.
1016 Recapitulation of Human Retinal Development from Human Pluripotent Stem Cells
1017 Generates Transplantable Populations of Cone Photoreceptors. *Stem Cell Reports*
1018 2017;9:820–37. <https://doi.org/10.1016/j.stemcr.2017.07.022>.
- 1019 [63] Lowe A, Harris R, Bhansali P, Cvekl A, Liu W. Intercellular Adhesion-Dependent Cell
1020 Survival and ROCK-Regulated Actomyosin-Driven Forces Mediate Self-Formation of a

- 1021 Retinal Organoid. *Stem Cell Reports* 2016;6:743–56.
- 1022 <https://doi.org/10.1016/j.stemcr.2016.03.011>.
- 1023 [64] Kim S, Lowe A, Dharmat R, Lee S, Owen LA, Wang J, et al. Generation, transcriptome
- 1024 profiling, and functional validation of cone-rich human retinal organoids. *Proc Natl Acad*
- 1025 *Sci U S A* 2019;166:10824–33. <https://doi.org/10.1073/pnas.1901572116>.
- 1026 [65] Gao ML, Lei XL, Han F, He KW, Jin SQ, Zhang YY, et al. Patient-Specific Retinal
- 1027 Organoids Recapitulate Disease Features of Late-Onset Retinitis Pigmentosa. *Front Cell*
- 1028 *Dev Biol* 2020;8:1–14. <https://doi.org/10.3389/fcell.2020.00128>.
- 1029 [66] Capowski EE, Samimi K, Mayerl SJ, Phillips MJ, Pinilla I, Howden SE, et al.
- 1030 Reproducibility and staging of 3D human retinal organoids across multiple pluripotent
- 1031 stem cell lines. *Development* 2019;146:dev171686. <https://doi.org/10.1242/dev.171686>.
- 1032 [67] Wahlin KJ, Maruotti JA, Sripathi SR, Ball J, Angueyra JM, Kim C, et al. Photoreceptor
- 1033 Outer Segment-like Structures in Long-Term 3D Retinas from Human Pluripotent Stem
- 1034 Cells. *Sci Rep* 2017;7:766. <https://doi.org/10.1038/s41598-017-00774-9>.
- 1035 [68] Regent F, Chen HY, Kelley RA, Qu Z, Swaroop A, Li T. A simple and efficient method
- 1036 for generating human retinal organoids. *Mol Vis* 2020;26:97–105.
- 1037 [69] Ma H, Ding X-Q. Thyroid Hormone Signaling and Cone Photoreceptor Viability. In:
- 1038 Bowes Rickman C, LaVail MM, Anderson RE, Grimm C, Hollyfield J, Ash J, editors.
- 1039 *Retin. Degener. Dis.*, Cham: Springer International Publishing; 2016, p. 613–8.
- 1040 [70] Eldred KC, Hadyniak SE, Hussey KA, Brenerman B, Zhang P, Chamling X, et al. Thyroid
- 1041 hormone signaling specifies cone subtypes in human retinal organoids. *Science*
- 1042 2018;362:359950. <https://doi.org/10.1126/science.aau6348>.
- 1043 [71] Takata N, Abbey D, Fiore L, Acosta S, Feng R, Gil HJ, et al. An Eye Organoid Approach

- 1044 Identifies Six3 Suppression of R-spondin 2 as a Critical Step in Mouse Neuroretina
 1045 Differentiation. *Cell Rep* 2017;21:1534–49. <https://doi.org/10.1016/j.celrep.2017.10.041>.
- 1046 [72] Quinn PM, Buck TM, Mulder AA, Ohonin C, Alves CH, Vos RM, et al. Human iPSC-
 1047 Derived Retinas Recapitulate the Fetal CRB1 CRB2 Complex Formation and Demonstrate
 1048 that Photoreceptors and Müller Glia Are Targets of AAV5. *Stem Cell Reports*
 1049 2019;12:906–19. <https://doi.org/10.1016/j.stemcr.2019.03.002>.
- 1050 [73] Capowski EE, Simonett JM, Clark EM, Wright LS, Howden SE, Wallace KA, et al. Loss
 1051 of MITF expression during human embryonic stem cell differentiation disrupts retinal
 1052 pigment epithelium development and optic vesicle cell proliferation. *Hum Mol Genet*
 1053 2014;23:6332–44. <https://doi.org/10.1093/hmg/ddu351>.
- 1054 [74] Bujakowska K, Audo I, Mohand-Säid S, Lancelot ME, Antonio A, Germain A, et al.
 1055 CRB1 mutations in inherited retinal dystrophies. *Hum Mutat* 2012;33:306–15.
 1056 <https://doi.org/10.1002/humu.21653>.
- 1057 [75] Quinn PM, Pellissier LP, Wijnholds J. The CRB1 complex: Following the trail of Crumbs
 1058 to a feasible gene therapy strategy. *Front Neurosci* 2017;11:175.
 1059 <https://doi.org/10.3389/FNINS.2017.00175>.
- 1060 [76] Quinn PMJ, Wijnholds J. Retinogenesis of the Human Fetal Retina: An Apical Polarity
 1061 Perspective. *Genes (Basel)* 2019;10:1–38. <https://doi.org/10.3390/genes10120987>.
- 1062 [77] Alves CH, Pellissier LP, Wijnholds J. The CRB1 and adherens junction complex proteins
 1063 in retinal development and maintenance. *Prog Retin Eye Res* 2014;40:35–52.
 1064 <https://doi.org/10.1016/j.preteyeres.2014.01.001>.
- 1065 [78] Talib M, van Schooneveld MJ, van Genderen MM, Wijnholds J, Florijn RJ, ten Brink JB,
 1066 et al. Genotypic and Phenotypic Characteristics of CRB1-Associated Retinal Dystrophies:

- 1067 A Long-Term Follow-up Study. *Ophthalmology* 2017;124:884–95.
1068 <https://doi.org/10.1016/j.opthta.2017.01.047>.
- 1069 [79] Aparicio JG, Hopp H, Choi A, Mandayam Comar J, Liao VC, Harutyunyan N, et al.
1070 Temporal expression of CD184(CXCR4) and CD171(L1CAM) identifies distinct early
1071 developmental stages of human retinal ganglion cells in embryonic stem cell derived
1072 retina. *Exp Eye Res* 2017;154:177–89. <https://doi.org/10.1016/j.exer.2016.11.013>.
- 1073 [80] Fligor CM, Langer KB, Sridhar A, Ren Y, Shields PK, Edler MC, et al. Three-
1074 Dimensional Retinal Organoids Facilitate the Investigation of Retinal Ganglion Cell
1075 Development, Organization and Neurite Outgrowth from Human Pluripotent Stem Cells.
1076 *Sci Rep* 2018;8:1–14. <https://doi.org/10.1038/s41598-018-32871-8>.
- 1077 [81] Kaewkhaw R, Kaya KD, Brooks M, Homma K, Zou J, Chaitankar V, et al. Transcriptome
1078 Dynamics of Developing Photoreceptors in Three-Dimensional Retina Cultures
1079 Recapitulates Temporal Sequence of Human Cone and Rod Differentiation Revealing Cell
1080 Surface Markers and Gene Networks. *Stem Cells* 2015;33:3504–18.
1081 <https://doi.org/10.1002/stem.2122>.
- 1082 [82] Hoshino A, Ratnapriya R, Brooks MJ, Chaitankar V, Wilken MS, Zhang C, et al.
1083 Molecular Anatomy of the Developing Human Retina. *Dev Cell* 2017;43:763-779.e4.
1084 <https://doi.org/10.1016/j.devcel.2017.10.029>.
- 1085 [83] Aldiri I, Xu B, Wang L, Chen X, Hiler D, Griffiths L, et al. The Dynamic Epigenetic
1086 Landscape of the Retina During Development, Reprogramming, and Tumorigenesis.
1087 *Neuron* 2017;94:550-568.e10. <https://doi.org/10.1016/j.neuron.2017.04.022>.
- 1088 [84] Collin J, Queen R, Zerti D, Dorgau B, Hussain R, Coxhead J, et al. Deconstructing Retinal
1089 Organoids: Single Cell RNA-Seq Reveals the Cellular Components of Human Pluripotent

- 1090 Stem Cell-Derived Retina. *Stem Cells* 2019;37:593–8. <https://doi.org/10.1002/stem.2963>.
- 1091 [85] Kallman A, Capowski EE, Wang J, Kaushik AM, Jansen AD, Edwards KL, et al.
 1092 Investigating cone photoreceptor development using patient-derived NRL null retinal
 1093 organoids. *Commun Biol* 2020;3:82. <https://doi.org/10.1038/s42003-020-0808-5>.
- 1094 [86] Marcucci F, Murcia-Belmonte V, Wang Q, Coca Y, Ferreiro-Galve S, Kuwajima T, et al.
 1095 The Ciliary Margin Zone of the Mammalian Retina Generates Retinal Ganglion Cells.
 1096 *Cell Rep* 2016;17:3153–64. <https://doi.org/10.1016/j.celrep.2016.11.016>.
- 1097 [87] Bélanger M-C, Robert B, Cayouette M. Msx1-Positive Progenitors in the Retinal Ciliary
 1098 Margin Give Rise to Both Neural and Non-neural Progenies in Mammals. *Dev Cell*
 1099 2017;40:137–50. <https://doi.org/10.1016/j.devcel.2016.11.020>.
- 1100 [88] Tropepe V, Coles BLK, Chiasson BJ, Horsford DJ, Elia AJ, McInnes RR, et al. Retinal
 1101 stem cells in the adult mammalian eye. *Science* (80-) 2000;287:2032–6.
 1102 <https://doi.org/10.1126/science.287.5460.2032>.
- 1103 [89] Kuwahara A, Ozone C, Nakano T, Saito K, Eiraku M, Sasai Y. Generation of a ciliary
 1104 margin-like stem cell niche from self-organizing human retinal tissue. *Nat Commun*
 1105 2015;6. <https://doi.org/10.1038/ncomms7286>.
- 1106 [90] Parfitt DA, Lane A, Ramsden CM, Carr AJF, Munro PM, Jovanovic K, et al.
 1107 Identification and Correction of Mechanisms Underlying Inherited Blindness in Human
 1108 iPSC-Derived Optic Cups. *Cell Stem Cell* 2016;18:769–81.
 1109 <https://doi.org/10.1016/j.stem.2016.03.021>.
- 1110 [91] Shimada H, Lu Q, Insinna-Kettenhofen C, Nagashima K, English MA, Semler EM, et al.
 1111 In Vitro Modeling Using Ciliopathy-Patient-Derived Cells Reveals Distinct Cilia
 1112 Dysfunctions Caused by CEP290 Mutations. *Cell Rep* 2017;20:384–96.

- 1113 <https://doi.org/10.1016/j.celrep.2017.06.045>.
- 1114 [92] Li G, Gao G, Wang P, Song X, Xu P, Xie B, et al. Generation and Characterization of
 1115 Induced Pluripotent Stem Cells and Retinal Organoids From a Leber's Congenital
 1116 Amaurosis Patient With Novel RPE65 Mutations. *Front Mol Neurosci* 2019;12:1–16.
 1117 <https://doi.org/10.3389/fnmol.2019.00212>.
- 1118 [93] Lukovic D, Artero Castro A, Kaya KD, Munezero D, Gieser L, Davó-Martínez C, et al.
 1119 Retinal Organoids derived from hiPSCs of an AIPL1-LCA Patient Maintain
 1120 Cytoarchitecture despite Reduced levels of Mutant AIPL1. *Sci Rep* 2020;10:1–13.
 1121 <https://doi.org/10.1038/s41598-020-62047-2>.
- 1122 [94] Deng WL, Gao ML, Lei XL, Lv JN, Zhao H, He KW, et al. Gene Correction Reverses
 1123 Ciliopathy and Photoreceptor Loss in iPSC-Derived Retinal Organoids from Retinitis
 1124 Pigmentosa Patients. *Stem Cell Reports* 2018;10:1267–81.
 1125 <https://doi.org/10.1016/j.stemcr.2018.02.003>.
- 1126 [95] van de Pavert SA, Kantardzhieva A, Malysheva A, Meuleman J, Versteeg I, Levelt C, et
 1127 al. Crumbs homologue 1 is required for maintenance of photoreceptor cell polarization
 1128 and adhesion during light exposure. *J Cell Sci* 2004;117:4169–77.
 1129 <https://doi.org/10.1242/jcs.01301>.
- 1130 [96] Van De Pavert SA, Meuleman J, Malysheva A, Aartsen WM, Versteeg I, Tonagel F, et al.
 1131 A single amino acid substitution (Cys249Trp) in Crb1 causes retinal degeneration and
 1132 deregulates expression of pituitary tumor transforming gene Pttg1. *J Neurosci*
 1133 2007;27:564–73. <https://doi.org/10.1523/JNEUROSCI.3496-06.2007>.
- 1134 [97] Guo Y, Wang P, Ma JH, Cui Z, Yu Q, Liu S, et al. Modeling Retinitis Pigmentosa: Retinal
 1135 Organoids Generated From the iPSCs of a Patient With the USH2A Mutation Show Early

- 1136 Developmental Abnormalities. *Front Cell Neurosci* 2019;13:1–17.
- 1137 <https://doi.org/10.3389/fncel.2019.00361>.
- 1138 [98] Buskin A, Zhu L, Chichagova V, Basu B, Mozaffari-Jovin S, Dolan D, et al. Disrupted
1139 alternative splicing for genes implicated in splicing and ciliogenesis causes PRPF31
1140 retinitis pigmentosa. *Nat Commun* 2018;9. <https://doi.org/10.1038/s41467-018-06448-y>.
- 1141 [99] Lane A, Jovanovic K, Shortall C, Ottaviani D, Panes AB, Schwarz N, et al. Modeling and
1142 Rescue of RP2 Retinitis Pigmentosa Using iPSC-Derived Retinal Organoids. *Stem Cell*
1143 *Reports* 2020;15:67–79. <https://doi.org/10.1016/j.stemcr.2020.05.007>.
- 1144 [100] VanderWall KB, Huang KC, Pan Y, Lavekar SS, Fligor CM, Allsop AR, et al. Retinal
1145 Ganglion Cells With a Glaucoma OPTN(E50K) Mutation Exhibit Neurodegenerative
1146 Phenotypes when Derived from Three-Dimensional Retinal Organoids. *Stem Cell Reports*
1147 2020;15:52–66. <https://doi.org/10.1016/j.stemcr.2020.05.009>.
- 1148 [101] Huang KC, Wang ML, Chen SJ, Kuo JC, Wang WJ, Nhi Nguyen PN, et al. Morphological
1149 and Molecular Defects in Human Three-Dimensional Retinal Organoid Model of X-
1150 Linked Juvenile Retinoschisis. *Stem Cell Reports* 2019;13:906–23.
1151 <https://doi.org/10.1016/j.stemcr.2019.09.010>.
- 1152 [102] Saengwimol D, Rojanaporn D, Chaitankar V, Chittavanich P, Aroonroch R, Boontawon
1153 T, et al. A three-dimensional organoid model recapitulates tumorigenic aspects and drug
1154 responses of advanced human retinoblastoma. *Sci Rep* 2018;8:1–13.
1155 <https://doi.org/10.1038/s41598-018-34037-y>.
- 1156 [103] Zheng C, Schneider JW, Hsieh J. Role of RB1 in human embryonic stem cell-derived
1157 retinal organoids. *Dev Biol* 2020. <https://doi.org/10.1016/j.ydbio.2020.03.011>.
- 1158 [104] Bai J, Wang C. Organoids and Microphysiological Systems: New Tools for Ophthalmic

- 1159 Drug Discovery. *Front Pharmacol* 2020;11:1–7. <https://doi.org/10.3389/fphar.2020.00407>.
- 1160 [105] Aasen DM, Vergara MN. New Drug Discovery Paradigms for Retinal Diseases: A Focus
1161 on Retinal Organoids. *J Ocul Pharmacol Ther* 2019;00:1–7.
1162 <https://doi.org/10.1089/jop.2018.0140>.
- 1163 [106] Cora V, Haderspeck J, Antkowiak L, Mattheus U, Neckel PH, Mack AF, et al. A Cleared
1164 View on Retinal Organoids. *Cells* 2019;8:391. <https://doi.org/10.3390/cells8050391>.
- 1165 [107] Ito S, Onishi A, Takahashi M. Chemically-induced photoreceptor degeneration and
1166 protection in mouse iPSC-derived three-dimensional retinal organoids. *Stem Cell Res*
1167 2017;24:94–101. <https://doi.org/10.1016/j.scr.2017.08.018>.
- 1168 [108] Kruczek K, Gonzalez-Cordero A, Goh D, Naeem A, Jonikas M, Blackford SJI, et al.
1169 Differentiation and Transplantation of Embryonic Stem Cell-Derived Cone Photoreceptors
1170 into a Mouse Model of End-Stage Retinal Degeneration. *Stem Cell Reports* 2017;8:1659–
1171 74. <https://doi.org/10.1016/j.stemcr.2017.04.030>.
- 1172 [109] McLelland BT, Lin B, Mathur A, Aramant RB, Thomas BB, Nistor G, et al. Transplanted
1173 hESC-derived retina organoid sheets differentiate, integrate, and improve visual function
1174 in retinal degenerate rats. *Investig Ophthalmol Vis Sci* 2018;59:2586–603.
1175 <https://doi.org/10.1167/iovs.17-23646>.
- 1176 [110] Iraha S, Tu HY, Yamasaki S, Kagawa T, Goto M, Takahashi R, et al. Establishment of
1177 Immunodeficient Retinal Degeneration Model Mice and Functional Maturation of Human
1178 ESC-Derived Retinal Sheets after Transplantation. *Stem Cell Reports* 2018;10:1059–74.
1179 <https://doi.org/10.1016/j.stemcr.2018.01.032>.
- 1180 [111] Gagliardi G, Ben M'Barek K, Chaffiol A, Slembrouck-Brec A, Conart JB, Nanteau C, et
1181 al. Characterization and Transplantation of CD73-Positive Photoreceptors Isolated from

- 1182 Human iPSC-Derived Retinal Organoids. *Stem Cell Reports* 2018;11:665–80.
 1183 <https://doi.org/10.1016/j.stemcr.2018.07.005>.
- 1184 [112] Eastlake K, Wang W, Jayaram H, Murray-Dunning C, Carr AJF, Ramsden CM, et al.
 1185 Phenotypic and Functional Characterization of Müller Glia Isolated from Induced
 1186 Pluripotent Stem Cell-Derived Retinal Organoids: Improvement of Retinal Ganglion Cell
 1187 Function upon Transplantation. *Stem Cells Transl Med* 2019:1–10.
 1188 <https://doi.org/10.1002/sctm.18-0263>.
- 1189 [113] Miltner AM, La Torre A. Retinal Ganglion Cell Replacement: Current Status and
 1190 Challenges Ahead. *Dev Dyn* 2019;248:118–28. <https://doi.org/10.1002/dvdy.24672>.
- 1191 [114] Santos-Ferreira T, Llonch S, Borsch O, Postel K, Haas J, Ader M. Retinal transplantation
 1192 of photoreceptors results in donor-host cytoplasmic exchange. *Nat Commun*
 1193 2016;7:13028. <https://doi.org/10.1038/ncomms13028>.
- 1194 [115] Pearson RA, Gonzalez-Cordero A, West EL, Ribeiro JR, Aghaizu N, Goh D, et al. Donor
 1195 and host photoreceptors engage in material transfer following transplantation of post-
 1196 mitotic photoreceptor precursors. *Nat Commun* 2016;7:13029.
 1197 <https://doi.org/10.1038/ncomms13029>.
- 1198 [116] Singh MS, Balmer J, Barnard AR, Aslam SA, Moralli D, Green CM, et al. Transplanted
 1199 photoreceptor precursors transfer proteins to host photoreceptors by a mechanism of
 1200 cytoplasmic fusion. *Nat Commun* 2016;7:13537. <https://doi.org/10.1038/ncomms13537>.
- 1201 [117] Pearson RA, Barber AC, Rizzi M, Hippert C, Xue T, West EL, et al. Restoration of vision
 1202 after transplantation of photoreceptors. *Nature* 2012;485:99–103.
 1203 <https://doi.org/10.1038/nature10997>.
- 1204 [118] Santos-Ferreira T, Postel K, Stutzki H, Kurth T, Zeck G, Ader M. Daylight vision repair

- 1205 by cell transplantation. *Stem Cells* 2015;33:79–90. <https://doi.org/10.1002/stem.1824>.
- 1206 [119] Santos-Ferreira TF, Borsch O, Ader M. Rebuilding the Missing Part—A Review on
1207 Photoreceptor Transplantation. *Front Syst Neurosci* 2017;10:1–14.
1208 <https://doi.org/10.3389/fnsys.2016.00105>.
- 1209 [120] Tu HY, Watanabe T, Shirai H, Yamasaki S, Kinoshita M, Matsushita K, et al. Medium- to
1210 long-term survival and functional examination of human iPSC-derived retinas in rat and
1211 primate models of retinal degeneration. *EBioMedicine* 2019;39:562–74.
1212 <https://doi.org/10.1016/j.ebiom.2018.11.028>.
- 1213 [121] Liu S, Xie B, Song X, Zheng D, He L, Li G, et al. Self-Formation of RPE Spheroids
1214 Facilitates Enrichment and Expansion of hiPSC-Derived RPE Generated on Retinal
1215 Organoid Induction Platform. *Invest Ophthalmol Vis Sci* 2018;59:5659–69.
1216 <https://doi.org/10.1167/iovs.17-23613>.
- 1217 [122] Wang N, Tosi J, Kasanuki JM, Chou CL, Kong J, Parmalee N, et al. Transplantation of
1218 reprogrammed embryonic stem cells improves visual function in a mouse model for
1219 retinitis pigmentosa. *Transplantation* 2010;89:911–9.
1220 <https://doi.org/10.1097/TP.0b013e3181d45a61>.
- 1221 [123] Li Y, Tsai YT, Hsu CW, Erol D, Yang J, Wu WH, et al. Long-term safety and efficacy of
1222 human-induced pluripotent stem cell (iPS) grafts in a preclinical model of retinitis
1223 pigmentosa. *Mol Med* 2012;18:1312–9. <https://doi.org/10.2119/molmed.2012.00242>.
- 1224 [124] Mehat MS, Sundaram V, Ripamonti C, Robson AG, Smith AJ, Borooah S, et al.
1225 Transplantation of Human Embryonic Stem Cell-Derived Retinal Pigment Epithelial Cells
1226 in Macular Degeneration. *Ophthalmology* 2018;125:1765–75.
1227 <https://doi.org/10.1016/j.ophtha.2018.04.037>.

- 1228 [125] Jiang DJ, Xu CL, Tsang SH. Revolution in gene medicine therapy and genome surgery.
 1229 Genes (Basel) 2018;9:2177–88. <https://doi.org/0.1172/JCI120429>.
- 1230 [126] Quinn PM, Buck TM, Ohonin C, Mikkers HMM, Wijnholds J. Production of iPS-Derived
 1231 Human Retinal Organoids for Use in Transgene Expression Assays. *Methods Mol Biol*
 1232 2018;1715:261–73. https://doi.org/10.1007/978-1-4939-7522-8_19.
- 1233 [127] Gonzalez Cordero A, Goh D, Kruczek K, Naeem A, Fernando M, kleine Holthaus S-M, et
 1234 al. Assessment of AAV vector tropisms for mouse and human pluripotent stem cell-
 1235 derived RPE and photoreceptor cells. *Hum Gene Ther* 2018;00:hum.2018.027.
 1236 <https://doi.org/10.1089/hum.2018.027>.
- 1237 [128] Garita-Hernandez M, Routet F, Guibbal L, Khabou H, Toualbi L, Riancho L, et al. AAV-
 1238 Mediated Gene Delivery to 3D Retinal Organoids Derived from Human Induced
 1239 Pluripotent Stem Cells. *Int J Mol Sci* 2020;21:994. <https://doi.org/10.3390/ijms21030994>.
- 1240 [129] Madeira MH, Boia R, Santos PF, Ambrósio AF, Santiago AR. Contribution of microglia-
 1241 mediated neuroinflammation to retinal degenerative diseases. *Mediators Inflamm*
 1242 2015;2015:673090. <https://doi.org/10.1155/2015/673090>.
- 1243 [130] van der Helm MW, van der Meer AD, Eijkel JCT, van den Berg A, Segerink LI.
 1244 Microfluidic organ-on-chip technology for blood-brain barrier research. *Tissue Barriers*
 1245 2016. <https://doi.org/10.1080/21688370.2016.1142493>.
- 1246 [131] Cunha-Vaz J, Bernardes R, Lobo C. Blood-retinal barrier. *Eur J Ophthalmol* 2011.
 1247 <https://doi.org/10.5301/EJO.2010.6049>.
- 1248 [132] Chen LJ, Ito S, Kai H, Nagamine K, Nagai N, Nishizawa M, et al. Microfluidic co-
 1249 cultures of retinal pigment epithelial cells and vascular endothelial cells to investigate
 1250 choroidal angiogenesis. *Sci Rep* 2017;7:1–9. <https://doi.org/10.1038/s41598-017-03788-5>.

- 1251 [133] Chung M, Lee S, Lee BJ, Son K, Jeon NL. Wet-AMD on a Chip : Modeling Outer Blood-
1252 Retinal Barrier In Vitro 2018;1700028:1–7. <https://doi.org/10.1002/adhm.201700028>.
- 1253 [134] Yeste J, García-Ramírez M, Illa X, Guimerà A, Hernández C, Simó R, et al. A
1254 compartmentalized microfluidic chip with crisscross microgrooves and
1255 electrophysiological electrodes for modeling the blood-retinal barrier. Lab Chip 2018.
1256 <https://doi.org/10.1039/c7lc00795g>.
- 1257 [135] Achberger K, Probst C, Haderspeck J, Bolz SS, Rogal J, Chuchuy J, et al. Merging
1258 organoid and organ-on-a-chip technology to generate complex multi-layer tissue models
1259 in a human retina-on-a-chip platform. Elife 2019;8:1–26.
1260 <https://doi.org/10.7554/elife.46188>.
- 1261 [136] Peng Z, Zhou L, Wong JKW, Chan YK. Eye-on-a-chip (EOC) models and their role in the
1262 future of ophthalmic drug discovery. Expert Rev Ophthalmol 2020;00:1–3.
1263 <https://doi.org/10.1080/17469899.2020.1788388>.
- 1264 [137] Chen PM, Gombart ZJ, Chen JW. Chloroquine treatment of ARPE-19 cells leads to
1265 lysosome dilation and intracellular lipid accumulation: Possible implications of lysosomal
1266 dysfunction in macular degeneration. Cell Biosci 2011;1:1–10.
1267 <https://doi.org/10.1186/2045-3701-1-10>.
- 1268 [138] Gonzalez MA, Flynn HW, Smiddy WE, Albini T, Berrocal AM, Tenzel P. Giant retinal
1269 tears after prior pars plana vitrectomy: Management strategies and outcomes. Clin
1270 Ophthalmol 2013;7:20130826. <https://doi.org/10.2147/OPHTH.S48930>.
- 1271 [139] Garnier S, Rahmi A, Grasswil C, Kodjikian L. Three hundred and sixty degree retinotomy
1272 for retinal detachments with severe proliferative vitreoretinopathy. Graefe's Arch Clin
1273 Exp Ophthalmol 2013;251:2081–5. <https://doi.org/10.1007/s00417-013-2298-3>.

- 1274 [140] Chan YK, Sy KHS, Wong CY, Man PK, Wong D, Shum HC. In vitro modeling of
1275 emulsification of silicone oil as intraocular tamponade using microengineered eye-on-a-
1276 chip. *Investig Ophthalmol Vis Sci* 2015;56:3314–9. [https://doi.org/10.1167/iovs.15-](https://doi.org/10.1167/iovs.15-16728)
1277 16728.
- 1278 [141] Norden C, Lecaudey V. Collective cell migration: general themes and new paradigms.
1279 *Curr Opin Genet Dev* 2019;57:54–60. <https://doi.org/10.1016/j.gde.2019.06.013>.
- 1280 [142] Mishra S, Thakur A, Redenti S, Vazquez M. A model microfluidics-based system for the
1281 human and mouse retina. *Biomed Microdevices* 2015;17. [https://doi.org/10.1007/s10544-](https://doi.org/10.1007/s10544-015-0002-6)
1282 015-0002-6.
- 1283 [143] Thakur A, Mishra S, Pena J, Zhou J, Redenti S, Majeska R, et al. Collective adhesion and
1284 displacement of retinal progenitor cells upon extracellular matrix substrates of
1285 transplantable biomaterials. *J Tissue Eng* 2018;9.
1286 <https://doi.org/10.1177/2041731417751286>.
- 1287 [144] Pena, Zhang, Majeska, Venkatesh, Vazquez. Invertebrate Retinal Progenitors as
1288 Regenerative Models in a Microfluidic System. *Cells* 2019;8:1301.
1289 <https://doi.org/10.3390/cells8101301>.
- 1290 [145] Mishra S, Peña JS, Redenti S, Vazquez M. A novel electro-chemotactic approach to
1291 impact the directional migration of transplantable retinal progenitor cells. *Exp Eye Res*
1292 2019;185:107688. <https://doi.org/10.1016/j.exer.2019.06.002>.
- 1293 [146] Huang FL, Russell P, Kuwabara T. Fine structure of lentoid bodies derived from normal
1294 and cataractous mouse lenses. *Exp Eye Res* 1980;31:535–41.
1295 [https://doi.org/10.1016/S0014-4835\(80\)80012-1](https://doi.org/10.1016/S0014-4835(80)80012-1).
- 1296 [147] Yang C, Yang Y, Brennan L, Bouhassira EE, Kantorow M, Cvekl A. Efficient generation

- 1297 of lens progenitor cells and lentoid bodies from human embryonic stem cells in
 1298 chemically defined conditions. *FASEB J* 2010;24:3274–83. [https://doi.org/10.1096/fj.10-](https://doi.org/10.1096/fj.10-157255)
 1299 157255.
- 1300 [148] Fu Q, Qin Z, Jin X, Zhang L, Chen Z, He J, et al. Generation of functional lentoid bodies
 1301 from human induced pluripotent stem cells derived from urinary cells. *Investig*
 1302 *Ophthalmol Vis Sci* 2017;58:517–27. <https://doi.org/10.1167/iovs.16-20504>.
- 1303 [149] Fu Q, Qin Z, Zhang L, Lyu D, Tang Q, Yin H, et al. A New Long Noncoding RNA ALB
 1304 Regulates Autophagy by Enhancing the Transformation of LC3BI to LC3BII during
 1305 Human Lens Development. *Mol Ther - Nucleic Acids* 2017;9:207–17.
 1306 <https://doi.org/10.1016/j.omtn.2017.09.011>.
- 1307 [150] Qiu X, Yang J, Liu T, Jiang Y, Le Q, Lu Y. Efficient generation of lens progenitor cells
 1308 from cataract patient-specific induced pluripotent stem cells. *PLoS One* 2012;7.
 1309 <https://doi.org/10.1371/journal.pone.0032612>.
- 1310 [151] Han C, Li J, Wang C, Ouyang H, Ding X, Liu Y, et al. Wnt5a contributes to the
 1311 differentiation of human embryonic stem cells into lentoid bodies through the
 1312 noncanonical Wnt/Jnk signaling pathway. *Investig Ophthalmol Vis Sci* 2018;59:3449–60.
 1313 <https://doi.org/10.1167/iovs.18-23902>.
- 1314 [152] Qin Z, Zhang L, Lyu D, Li J, Tang Q, Yin H, et al. Opacification of lentoid bodies derived
 1315 from human induced pluripotent stem cells is accelerated by hydrogen peroxide and
 1316 involves protein aggregation. *J Cell Physiol* 2019;234:23750–62.
 1317 <https://doi.org/10.1002/jcp.28943>.
- 1318 [153] Murphy P, Kabir MH, Srivastava T, Mason ME, Dewi CU, Lim S, et al. Light-focusing
 1319 human micro-lenses generated from pluripotent stem cells model lens development and

- 1320 drug-induced cataract in vitro. *Dev* 2018;145. <https://doi.org/10.1242/dev.155838>.
- 1321 [154] Ali M, Kabir F, Thomson JJ, Ma Y, Qiu C, Delannoy M, et al. Comparative transcriptome
1322 analysis of hESC- and iPSC-derived lentoid bodies. *Sci Rep* 2019;9:1–9.
1323 <https://doi.org/10.1038/s41598-019-54258-z>.
- 1324 [155] Di Zazzo A, Lee S-M, Sung J, Niutta M, Coassin M, Mashaghi A, et al. Variable
1325 Responses to Corneal Grafts: Insights from Immunology and Systems Biology. *J Clin*
1326 *Med* 2020. <https://doi.org/10.3390/jcm9020586>.
- 1327 [156] Kim J, Koo BK, Knoblich JA. Human organoids: model systems for human biology and
1328 medicine. *Nat Rev Mol Cell Biol* 2020. <https://doi.org/10.1038/s41580-020-0259-3>.
- 1329 [157] Junaid A, Mashaghi A, Hankemeier T, Vulto P. An end-user perspective on Organ-on-a-
1330 Chip: Assays and usability aspects. *Curr Opin Biomed Eng* 2017.
1331 <https://doi.org/10.1016/j.cobme.2017.02.002>.
- 1332 [158] Mashaghi A, Hong J, Chauhan SK, Dana R. Ageing and ocular surface immunity. *Br J*
1333 *Ophthalmol* 2017. <https://doi.org/10.1136/bjophthalmol-2015-307848>.
- 1334 [159] Inomata T, Mashaghi A, Hong J, Nakao T, Dana R. Scaling and maintenance of corneal
1335 thickness during aging. *PLoS One* 2017. <https://doi.org/10.1371/journal.pone.0185694>.
- 1336 [160] Tang H, Abouleila Y, Si L, Ortega-Prieto AM, Mummery CL, Ingber DE, et al. Human
1337 Organs-on-Chips for Virology. *Trends Microbiol* 2020.
1338 <https://doi.org/10.1016/j.tim.2020.06.005>.
- 1339 [161] Jalili-Firoozinezhad S, Gazzaniga FS, Calamari EL, Camacho DM, Fadel CW, Bein A, et
1340 al. A complex human gut microbiome cultured in an anaerobic intestine-on-a-chip. *Nat*
1341 *Biomed Eng* 2019. <https://doi.org/10.1038/s41551-019-0397-0>.
- 1342 [162] Heidari M, Noorizadeh F, Wu K, Inomata T, Mashaghi A. Dry Eye Disease: Emerging

- 1343 Approaches to Disease Analysis and Therapy. J Clin Med 2019.
1344 <https://doi.org/10.3390/jcm8091439>.
- 1345 [163] Di Zazzo A, Yang W, Coassin M, Micera A, Antonini M, Piccinni F, et al. Signaling
1346 lipids as diagnostic biomarkers for ocular surface cicatrizing conjunctivitis. J Mol Med
1347 2020. <https://doi.org/10.1007/s00109-020-01907-w>.
- 1348 [164] Caruso S, Ryu J, Quinn PMJ, Tsang SH. Precision metabolome reprogramming for
1349 imprecision therapeutics in retinitis pigmentosa. J Clin Invest 2020.
1350 <https://doi.org/10.1172/JCI139239>.
1351